

University of New Orleans

ScholarWorks@UNO

University of New Orleans Theses and
Dissertations

Dissertations and Theses

5-18-2007

Characterization of Structures and Deformation in the Brittle-Ductile Transition, Western Termination of the Chugach Metamorphic Complex, Southern Alaska

Erik Day

University of New Orleans

Follow this and additional works at: <https://scholarworks.uno.edu/td>

Recommended Citation

Day, Erik, "Characterization of Structures and Deformation in the Brittle-Ductile Transition, Western Termination of the Chugach Metamorphic Complex, Southern Alaska" (2007). *University of New Orleans Theses and Dissertations*. 529.

<https://scholarworks.uno.edu/td/529>

This Thesis is protected by copyright and/or related rights. It has been brought to you by ScholarWorks@UNO with permission from the rights-holder(s). You are free to use this Thesis in any way that is permitted by the copyright and related rights legislation that applies to your use. For other uses you need to obtain permission from the rights-holder(s) directly, unless additional rights are indicated by a Creative Commons license in the record and/or on the work itself.

This Thesis has been accepted for inclusion in University of New Orleans Theses and Dissertations by an authorized administrator of ScholarWorks@UNO. For more information, please contact scholarworks@uno.edu.

Characterization of Structures and Deformation in the Brittle-Ductile Transition, Western
Termination of the Chugach Metamorphic Complex, Southern Alaska

A Thesis

Submitted to the Graduate Faculty of the
University of New Orleans
in partial fulfillment of the
requirements for the degree of

Master of Science
in
Geology and Geophysics

by

Erik Day

B.A. Occidental College, 2003

May, 2007

TABLE OF CONTENTS

List of Figures.....	iii
Abstract.....	iv
Introduction.....	1
Body.....	2
Geologic Setting.....	2
Methods.....	7
Structural Data.....	8
West bank of Copper River canyon.....	11
Lower Bremner River section.....	14
Upper Bremner River section.....	16
Stuart Creek fault.....	17
Interpretation of Field Relationships.....	17
Interpretation of the Bremner shear zone and the Stuart Creek fault.....	18
EBSD Results.....	20
Petrographic Analysis.....	24
Discussion.....	26
Dislocation Creep in the CMC.....	26
The Importance of Rheology.....	28
Explanations for Observed Deformation.....	31
Pore Space.....	32
The Importance of Aluminum.....	33
Effects of Increased Pressure Solution.....	36
Summary and Conclusions.....	37
Future Work.....	39
References Cited.....	41
Appendices.....	45
Appendix A: Petrographic Sample Descriptions.....	45
Appendix B: Field Map Data.....	51
Vita.....	57

LIST OF FIGURES

Figure 1. Tectonic map of southern Alaska	2
Figure 2. Foliation map of area.....	4
Figure 3. Tectonic setting ~52ma	6
Figure 4. Teyssier et al. (2002) model summary	7
Figure 5. Cross sections	12
Figure 6. Orientation data	13
Figure 7. Vertical S2	14
Figure 8. Shallow to moderate S2.....	15
Figure 9. Block diagram of the Bremner foliation fan.....	20
Figure 10. EBSD pole figures.....	21
Figure 11. Shear sense via S/C relationships.....	26
Figure 12. Strain rate versus temperature diagram	29
Figure 13. Uplift Mechanism.....	40
Table 1. Fabric Summary.....	10
Table 2. Shear sense data.....	25

ABSTRACT

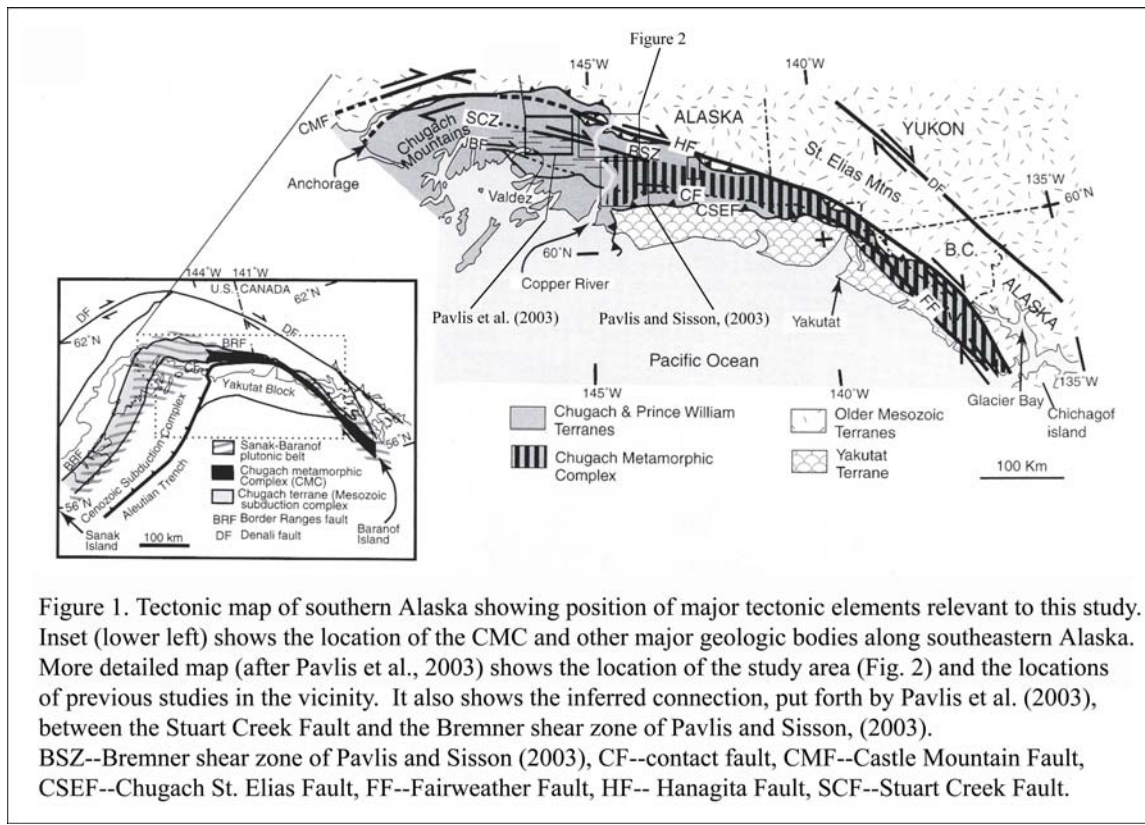
Field mapping along the western termination of the Chugach Metamorphic Complex (CMC) revealed a new D2 structure, the Bremner foliation fan. This structure has a high strain, vertically foliated core, with moderate-shallow dipping cleavages to the north and south which rollover into the core. The fan appears to have propagated from below by a shear-zone at depth (O'Driscoll, 2006). Description of the Bremner foliation fan revealed that the Bremner shear zone of Pavlis and Sisson (2003) is a D3 structure, and that the Stuart Creek fault is a younger brittle fault with 90km of dextral offset. Electron Back Scatter Diffraction (EBSD) and microstructural observations revealed deformation mechanisms were primarily compositionally controlled, whereas P-T-t conditions played a secondary role. Other factors, deemed to be of lesser influence included increased pressure solution caused by high fluid mobility, a lack of pore space, high levels of free aluminum, and a load-bearing framework of phyllosilicates.

INTRODUCTION

The western termination of the the Chugach Metamorphic Complex (CMC) is a complex zone of transpressional deformation structures developed within the forearc of the eastern Aleutian arc-trench system. The CMC had been mapped decades ago (eg. Hudson and Plafker, 1982) on a large scale (Fig. 1), but more detailed studies have only recently begun to show the tectonic processes that have generated the complex. A study by Pavlis and Sisson (2003) described the foliation pattern created by a strike slip shear zone, named the Bremner shear zone, passing downward from lower-grade schists through to high grade gneisses (Fig. 2). They compared the structure of their shear zone to a model presented by Teyssier et al. (2002), where a brittle upper crust moved over a ductile middle crust. As depth increased, accumulated strain was evenly distributed into a lower gneissic zone. The work presented here was carried out with the intention of extending the mapped area of the Bremner shear zone of Pavlis and Sisson (2003), and testing the application of Teyssier et al.'s (2002) model to this region (Fig 2). New structural data were collected (Appendix B: a, b, c, d, e) and cross sections were created (Fig. 5a, b, and c). Analysis of the new data and cross sections revealed a new and different shear zone than that identified by Pavlis and Sisson (2003). This new structure is a large foliation fan referred to here as the Bremner foliation fan and represents a distinct structure from the Bremner shear zone (Fig. 2). Identification of the fan provides the opportunity to clarify the history of deformation in the area, and to refine existing models of deformation in the CMC.

In this thesis, I describe a reanalysis of the Bremner shear zone, the Stuart Creek fault, and their relation to the Bremner foliation fan. These structures are discussed in terms of the deformational sequence and variation in metamorphic grade. Electron Back Scatter Diffraction (EBSD) and petrographic analysis of samples from the fan have been used to show the importance of variations in rheology in the structural evolution of the complex. Observations

show a mixed behavior of pressure solution and dynamic recrystallization deformation mechanisms where metagraywacke show dynamic recrystallization and metapelites show pressure solution and this relationship seems more dependent on lithology than metamorphic grade. Finally, I discuss how other variables, such as increased pressure solution caused by; high fluid mobility, a lack of pore space, high levels of free aluminum, and a load-bearing framework of phyllosilicates, affect the observed deformation pattern.



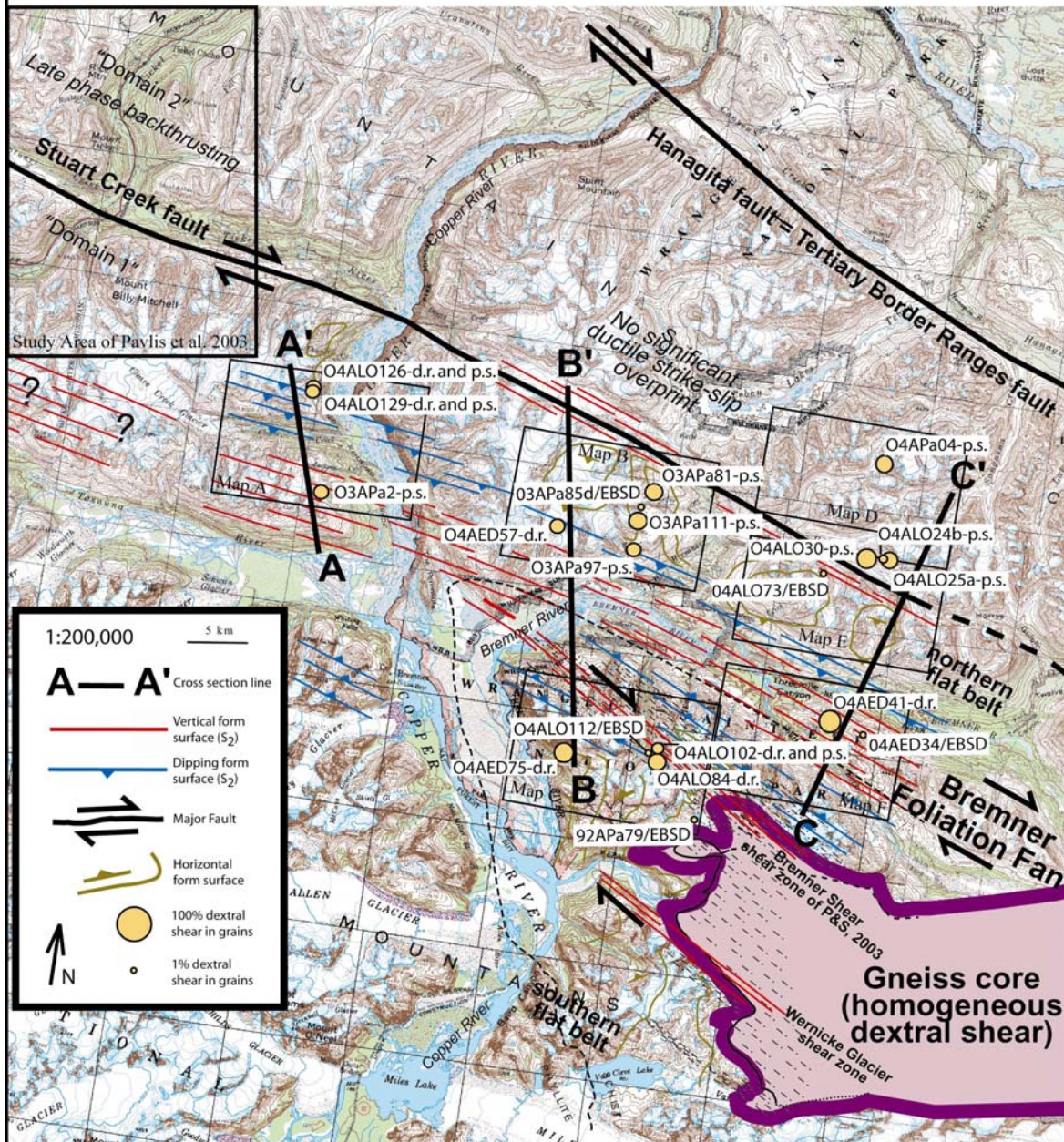
GEOLOGIC SETTING

The bulk of the rocks of the Chugach and Prince William Terranes were deposited as turbidite flows from the Late Cretaceous, Maastrichtian to early Tertiary, the source of which is thought to be the Coast Plutonic and metamorphic complex of SE Alaska (Plafker et al., 1994). These terranes were originally deposited in the trench off the coast of the Coast Mountains ranging from southeastern Alaska to British Columbia (Plafker et al., 1994). From the late

Cretaceous to Eocene the terranes were accreted by subduction and transported to the northwest to their current positions in southern Alaska via transpressional subduction. Later Eocene to Cenozoic subduction along the Alaskan-Aleutian arc uplifted and exposed the Chugach and Prince William terranes. While these terranes are separated lithologically, within them is a metamorphic belt referred to as the Chugach Metamorphic Complex (CMC) (Fig. 1) (Hudson and Plafker, 1982; Plafker et al., 1994; Pavlis and Sisson, 1995). The CMC, a part of this forearc accretionary complex, is composed primarily of the Cretaceous graywackes and argillites of the Valdez Group (Hudson and Plafker, 1982; Pavlis et al, 2003). The high temperature low pressure sub-greenschist to amphibolite facies metamorphism of the CMC has been explained as a result of the Kula-Farallon ridge subduction (Sisson et al, 1989; Sisson and Pavlis, 1993). The highest grade rocks at the core of the complex reached a maximum temperature of $\sim 650^{\circ}\text{C}$ and a maximum pressure of $\sim 4\text{kb}$ (Sisson et al. 1989). Lower grade rocks were deformed under temperatures between 300°C and 420°C and pressures between ~ 1 and 4 kb (Pavlis et al, 2003). This thermal event has been shown to have occurred at the same time as an Eocene dextral strike slip event associated with the overall oblique Alaskan-Aleutian arc subduction.

Oblique subduction and in particular subduction of transform and ridge sections of this former trench-ridge-trench oceanic plate boundary has shaped the structural style of the region and especially the CMC. Figure 3 (from Pavlis and Sisson, 1995) shows what the region may have looked like as the ridge subduction event transpired at $\sim 52\text{ Ma}$.

Figure 2: Structural map showing foliation patterns and other structures located along the western termination of the CMC. Inset boxes show locations of detailed mapwork. Locations of cross sections and new interpretations of the Stuart Creek fault and the Bremner shear zone of Pavlis and Sisson, (2003) are visible. Sample sites shown by orange circles, the size of the circle references the percent of dextral grains counted in each sample. Sample labels also show observed deformation mechanisms; d.r.- dynamic recrystallization, p.s.- pressure solution.

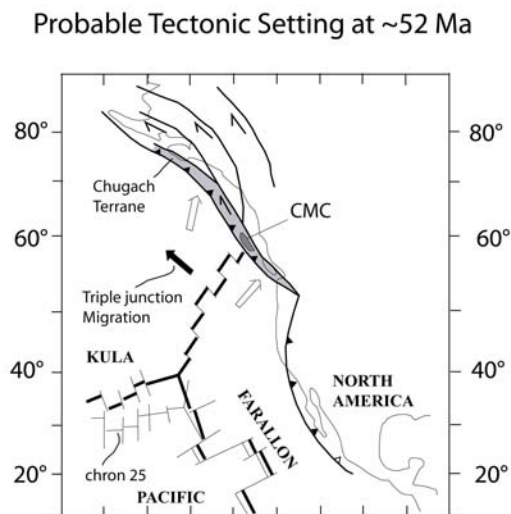


Previous work done in the area of the Copper River delta region has shown that there are three pervasive cleavages in the CMC (Pavlis and Sisson, 1995, 2003). Early interpretation of these cleavages described them as resulting from three distinct tectonic events. The first fabric, S₁, is cryptic and parallel to layering in the Valdez Group. This cleavage is described as a north-

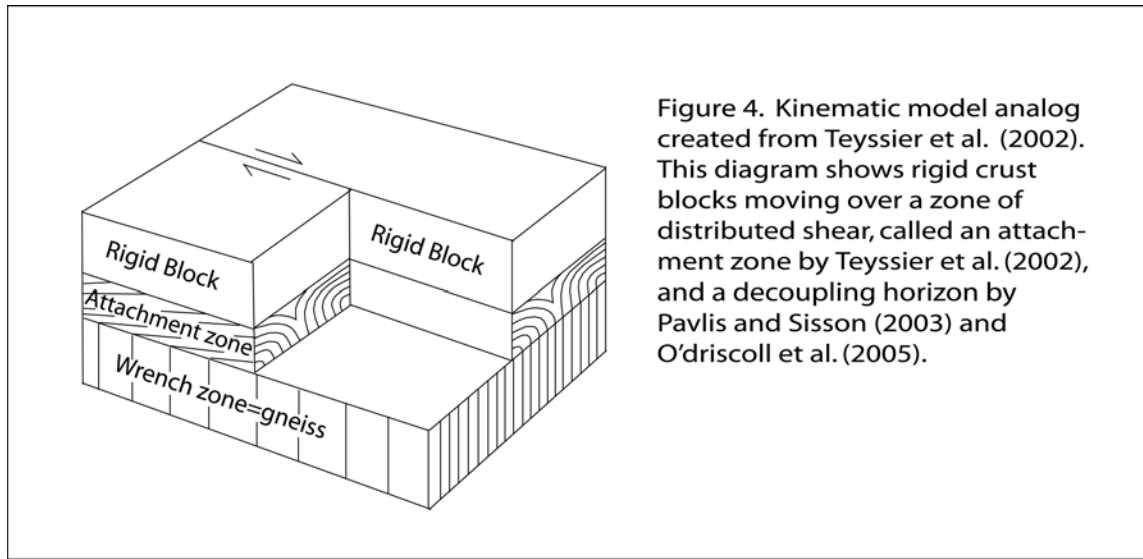
south shortening fabric associated with subduction related thrust faulting within the forming accretionary complex and produced a generally EW striking, steeply dipping phyllitic cleavage (Pavlis and Sisson, 1995; Pavlis and Sisson, 2003; Pavlis et al., 2003). S2 is shallow-dipping foliation in much of the CMC and represents the main continuous cleavage with an associated EW, shallow plunging elongation lineation (Pavlis and Sisson, 1995, 2003). Initially S2 was explained as a product of vertical shortening due to the subduction of the Kula-Farralon ridge, but in this study we document a more complex kinematic development for these D2 fabrics (Pavlis and Sisson, 1995). The third fabric, S3, is a vertical fabric which is observed overprinting the two previous fabrics (Pavlis and Sisson, 1995, 2003). This final fabric was initially explained as a result of the kinematic shifts following the passing of the Kula-Farallon ridge (Pavlis and Sisson, 1995). Pavlis and Sisson (2003) offered up a second interpretation for these last two fabrics, where S2 and S3 are the result of the same progressive deformational event.

Pavlis et al. (2003) described the region along the Richardson Highway as having two deformational domains (Fig. 2). “Domain 1” was dominated by 2 cleavages, showing constrictional finite strains interpreted as the result of a lengthening narrowing shear (terminology of Tikoff and Fossen, 1999). This zone was interpreted as the result of two events, the first was a thrusting event associated with an accretionary complex and the second event was a single constrictional strain event associated with the ductile section of a dextral strike slip fault. “Domain 2,” northeast of the Stuart Creek lineament, referred to as the Stuart Creek Fault in this work (Fig. 2), is stated to have a different kinematic history where D1 vertical thrusting is followed by D2 shearing, and finally a D3 back thrusting event.

Figure 3. Probable tectonic setting of the Chugach metamorphic complex in the early Eocene (After Pavlis and Sisson, 1995). Light shading shows Chugach terrane, darker shading shows location of the Chugach metamorphic belt.



O'Driscoll (2006) compared the foliation pattern of the western termination of the CMC to a model presented by Teyssier et al. (2002). This theory developed the concept of an attachment zone where a brittle upper crust moved over a ductile middle to lower crust where accumulated strain is evenly distributed in the rock (Fig. 4) (Teyssier et al., 2002; Pavlis and Sisson, 2003; O'Driscoll, 2006). O'Driscoll (2006) considered a modified version of Teyssier's model to explain the observed deformation in the CMC. This model, however, was unable to match the observed structural geometry. Thus, O'Driscoll (2006) proposed an "inverted attachment model" which more closely matched field observations. In this model, a deep shear zone was inferred beneath a mid-crustal zone of distributed shear (O'Driscoll, 2006). While this adjusted model is counterintuitive to the traditional views of the mechanical stratification of the lithosphere, it provided the best fit to field mapping and observation. I re-evaluate this model here.



METHODS

Field data were collected on foot from base camps established by helicopter during the summers of 2003 and 2004. Field mapping was done on hand-held Ipaq computers using the ESRI ArcPad mapping software and then later made into 1:42,000 scale maps using ESRI's ArcMap software. Rock samples were collected during these and previous field seasons with the intention of observing microstructures and textures.

Thin sections of samples were prepared by cutting parallel to lineation and perpendicular to foliation; and then examined with a petrographic microscope. In some samples, shear sense was estimated in thin sections, one hundred grains were counted per slide in order to determine a sense of shear using fabric asymmetries (delta and sigma porphyroclast shapes). The dominant deformation mechanism was also inferred using microstructures and textures that were identified under the petrographic microscope. Additional analysis was done using The University of New Orleans's Scanning Electron Microscope (S.E.M.), data collected with the S.E.M. supplemented the petrographic analysis and helped verify the petrographic mineral identifications.

Work at UNO was done with an AMRAY 1820 digital S.E.M. at 15kv acceleration potential, an 18 millimeter working distance, 400 micron final aperture, and a 60 second count time. Image capture was done with the program EDS2004 made by IXRF SYSTEMS Inc.

Electron Back Scatter Diffraction (EBSD) analysis was done using a S.E.M. owned by the Marine Biological Laboratory (MBL), and cooperatively used by Woods Hole Oceanographic Institute (WHOI). Work done in Woods Hole was done with a JEOL JSM-840 SEM with a tungsten filament, at 15kv acceleration potential, a 23 millimeter working distance, and a 70 micron final aperture. Data capture was done with the HKL Flamenco EBSD acquisition program, Version 5.0.8.0.

STRUCTURAL DATA

Field work and laboratory work were carried out to test two alternative hypotheses: 1) Pavlis and Sisson's (2003) suggestions that the Bremner shear zone (Fig. 2) connected up-dip to the Stuart Creek fault, essentially crossing a paleo-brittle ductile transition; or 2) an attachment hypothesis based on Teyssier et al.'s (2002) models which predict that the Bremner shear zone should disappear into a cleavage fan. During the course of our field work we discovered that neither hypothesis could be used to fully explain observations in the study area.

Figure 2 is a regional map that shows the geographic distribution of structural relationships observed during this study. The key observation that can be made from this map is that the Bremner shear zone of Pavlis and Sisson (2003) neither connects to a fault nor disappears into the D3 cleavage fan. Instead we observed a large scale structure that we have called the Bremner foliation fan that is distinct from the Bremner shear zone. The fan is a D2 structure and therefore older than the D3 Bremner shear zone and is defined by the large-scale geometry of the S2 foliation across the region.

We began our work near site 03APa2 (Fig. 2) just west of the Copper River because this area lay directly along strike from the Bremner shear zone of Pavlis and Sisson (2003). Its location along strike from the Bremner shear zone seemed key to distinguishing between our two working hypotheses. In this area we observed a prominent, ~EW striking, steeply dipping mica foliation with a strong subhorizontal stretching lineation recognized by both object shapes and crystallographic alignment. Based on this observation, the recognition of numerous dextral shear sense indicators, and the location of the area along strike from the Bremner shear zone it seemed likely that the steep fabric was a D3 fabric directly related to the Bremner shear zone.

As field work progressed, however, it became clear that these assumptions were wrong, and in retrospect the location we chose to begin our field work was a poor one because it produced significant confusion on fabric relationships. There were no overprinting relationships demonstrating that the steep foliation in this region was overprinting an earlier mica foliation; a characteristic of D2-D3 overprints elsewhere (Pavlis and Sisson, 2003). Instead, we recognized that the steep foliation in this area was the main mica foliation, a relationship more typical of D2 fabrics in the CMC, and the main mica foliation fanned to shallower south dips as we moved northward and shallower north dips as we moved southward away from the a steeply dipping core. This fanning of foliations can be seen in Figures 5a and 6a. The key observation, however, is that this fanning foliation is a D2 structure, and the Bremner shear zone is a distinct, younger (D3) structure that either merges with, or is distinct from, the large scale foliation fan. These fabric relations are summarized in Table 1.

In this section, I describe the general field observations that support this conclusion, describing structural relationships in three general mapping areas: 1) west of the Copper River

(section A-A', Fig. 5a); 2) lower Bremner River (section B-B', Fig. 5b); and 3) upper Bremner River (C-C', Fig. 5c).

TABLE 1. FABRIC SUMMARY

Fabric	Description	Kinematics
D3		
Folds (F3)	Tight to close, upright folding of S2 S1, and S0 with subhorizontal axes trending ~300°.	Dextral shear localized to areas of the Bremner shear zone of Pavlis and Sisson (2003) and the Wernicke Glacier shear zone.
Planar Fabrics (S3)	Main phyllitic cleavage is subvertical with ~300° strike; axial planar to F3 folds. Circled in red in Figure 6b.	
Linear Fabrics (L3)	Stretched pebbles, S2-S3 intersection lineation, subhorizontal, ~300° trend parallel to F3 axes. Circled in red in Figure 6b.	
D2		
Folds (F2)	Isoclinal to sub-isoclinal folds in the core of the fan, quickly open to close-tight folds as one moves N or S away from the core. Subhorizontal ~E-W axes	Dextral shear driven from below by a deeper strike slip shear zone (O'Driscoll, 2006)
Planar Fabrics (S2)	Main phyllitic cleavage is subvertical in the core of the Bremner foliation fan, but roll over to moderate to shallow S or N dips as one moves N or S respectively. ~E-W strike	
Linear Fabrics (L2)	Stretched pebbles, S1-S2 intersection lineation, subhorizontal, ~300° trend parallel to F2 axes	
D1		
Folds (F1)	Steeply inclined, subhorizontal to gently plunging, close to subisoclinal, south vergent folds	South directed thrusting
Planar Fabrics (S1)	Spaced phyllitic cleavage axial planar to F1 folds. Generally subparallel to layering (S0)	
Linear Fabrics (L1)	Bedding (S0)-Cleavage (S1) intersection	
D0		
Planar Fabrics (S0)	Bedding; graywacke and argillite	Late Cretaceous, Maastrichtian, to early Tertiary turbidite flows

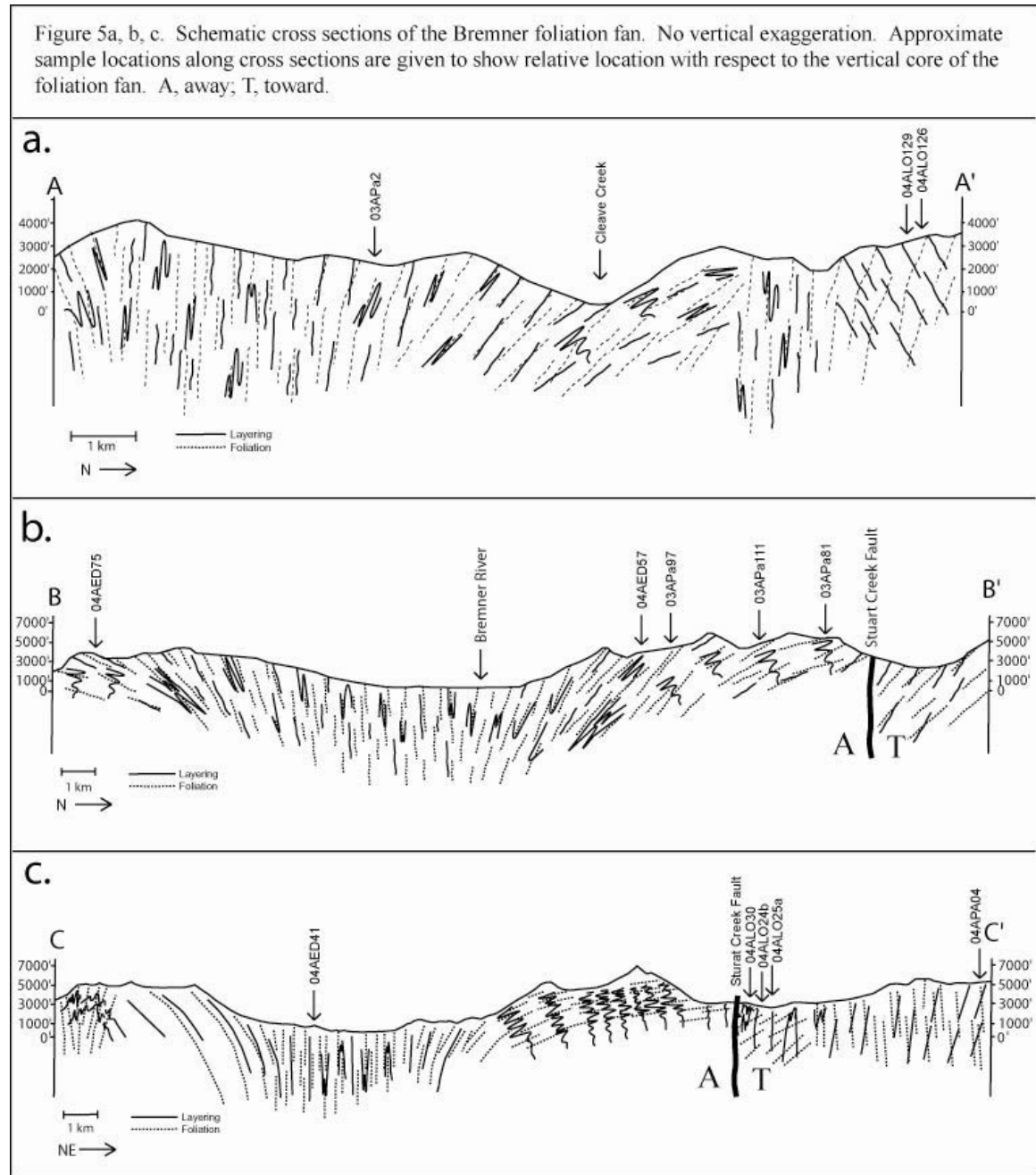
West bank of Copper River canyon

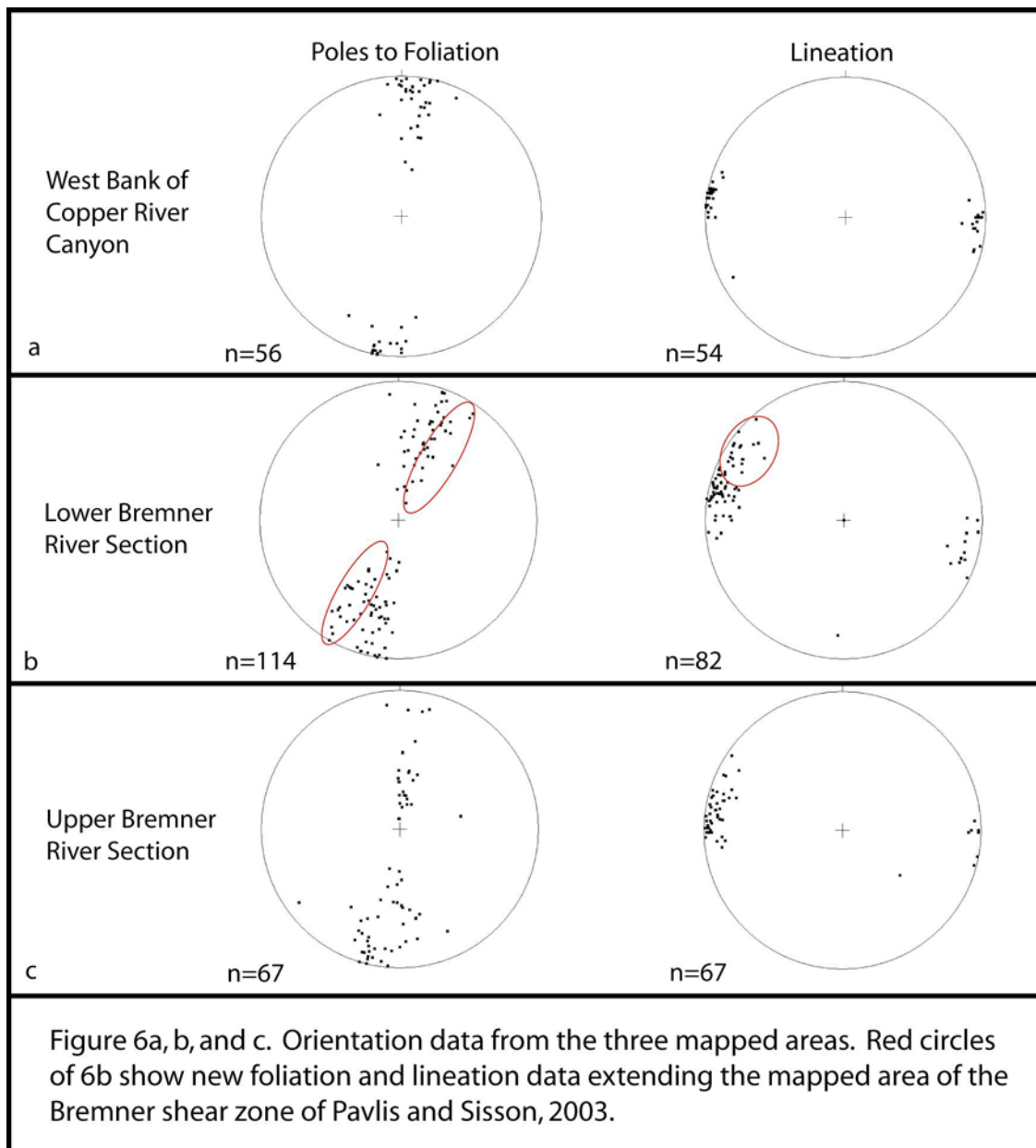
This area was examined by detailed mapping from two fly camps as well as helicopter reconnaissance at 3 sites away from the camps. Observations south of the Tasnuna River are limited to helicopter reconnaissance, but the northern part of this section (A-A', Fig. 5a) is well constrained by mapping.

The key feature of this region is that the Bremner foliation fan is well defined, but the structure becomes more cryptic away from the core of the zone, presumably due to lower finite strain in these low grade rocks. Specifically, in the steeply dipping core of the fan, layering and the principal mica foliation (S2) are virtually parallel, aside from the closures of large subisoclinal to isoclinal folds (Fig. 7, Appendix B: map A). The cleavage is a phyllitic cleavage marked primarily by fine-grained chlorite + biotite +/- white mica. Lineation is subhorizontal, and is clearly a stretching lineation as evidenced by deformed pebbles and argillite rip-up clasts observed at several localities (O'Driscoll, 2006). In accord with the layer parallel foliation, the finite strains indicated by deformed objects are clearly high (eg. Flinn plot X/Y:Y/Z ratios ranging from 1.25:1.25 to ~3.5:1.25, data collected by O'Driscoll, 2006) and largely transpose layering.

To the north of the steeply dipping core to the foliation fan, the mica foliation decreases to moderate and even low south-dips to define the fan (Fig. 5a) but the foliation diverges sharply from layering, which shows a characteristic gentle, to moderate north-dip throughout this area. Open to tight folds are present in layering in association with the foliation, but do not disturb the general north-dip of layering; i.e. D2 enveloping surfaces retain a moderate north dip, which is apparent by the map trace of layering (Fig. 8, Appendix B: Map A). To the south, we examined

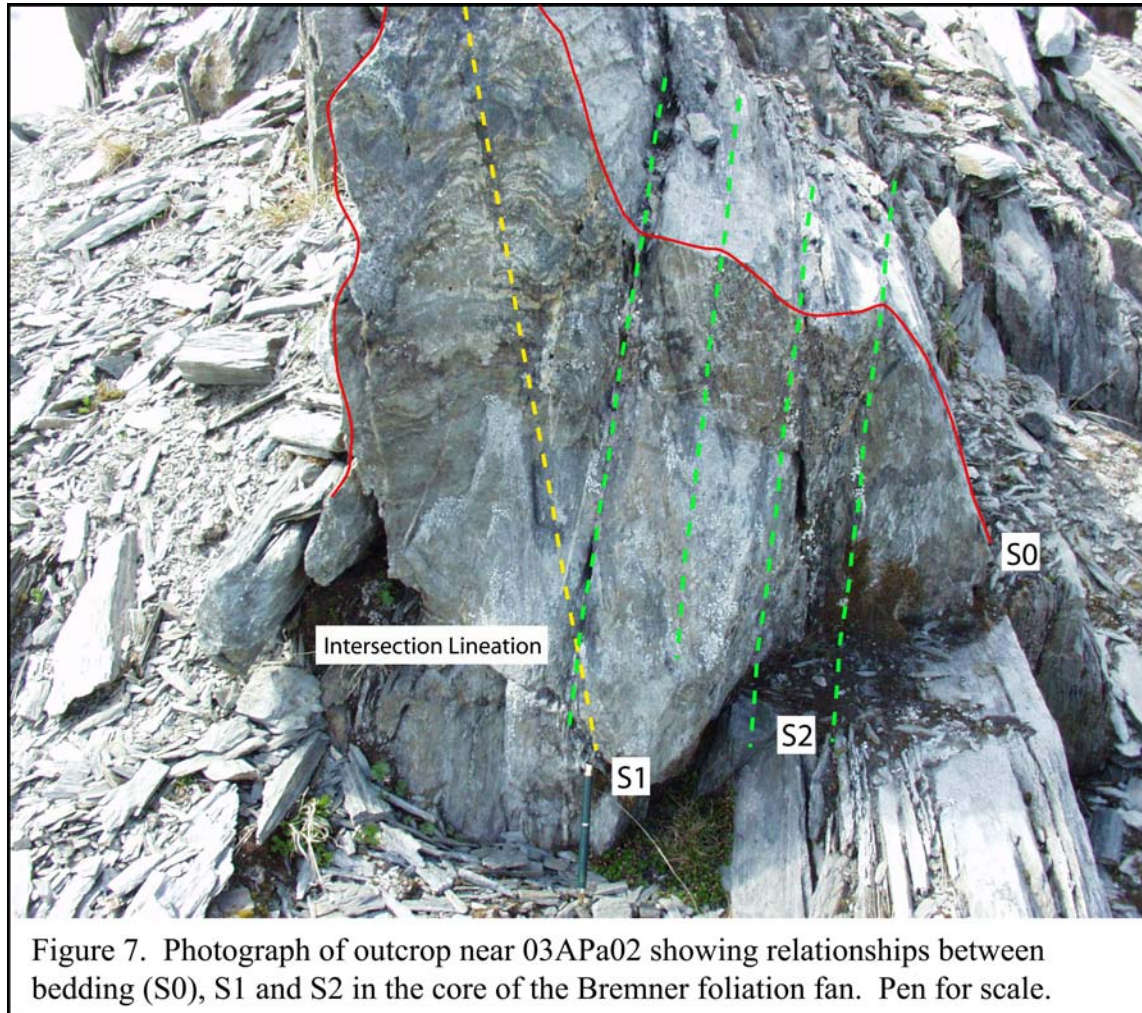
one site in reconnaissance work south of the Tasnuna River. In that area, a moderately north-dipping mica foliation is an S2 fabric that defines the southern part of the foliation fan.





Collectively, these observations demonstrate the basic fanning geometry of the S2 cleavage from the steeply dipping core of the zone to its margins (Fig. 5a and 6a). Interestingly, the S2 fabric appears to decrease in intensity away from the core of the foliation fan which is almost certainly also reflected as a decrease in finite strain. In addition, the S2 cleavage never reaches the very low-dips away from the fan that are observed farther east in lower-grade and higher-grade rocks; a relationship that has important implications for the regional geometry. In

contrast, farther west, this cleavage imprint becomes cryptic because a similar structural geometry was not recognized along the Richardson highway (Pavlis et al., 2003) or farther south (Nokleberg et al., 1989; Plafker et al., 1989).



Lower Bremner River section

This area was examined from three camps north of the Bremner River (Appendix B: map B) and two camps south of the Bremner River (Appendix B: map C), together with several helicopter spot observations and flybys. Thus, this segment of the foliation fan is probably the most well known part of the system.



As observed along the west side of the Copper River, a broad band of steeply dipping S2 cleavage with close to isoclinal folding of layering defines the core of the foliation fan in this segment (Fig. 5a and b). However, in this segment, the S2 cleavage defines a much more prominent fan, rolling to nearly horizontal dips to the south, and relatively shallow dips to the north. Moreover, F2 folds are prominent throughout the fan with isoclinal to subisoclinal F2 folds throughout the southern limb of the fan, and extending approximately 5km into the north flank of the fan as well. However, to the north of the fan there is a prominent decreasing strain gradient recorded in the geometry of F2 folds with F2 isoclinal folds opening rapidly northward until they are close to tight folds near the Stuart Creek fault (right side of figure 5b).

Reconnaissance mapping north of the Stuart Creek fault revealed moderate south dipping bedding and a layer parallel cleavage (S1), with little evidence of D2 overprinting.

The southern portion of this section also revealed foliation and lineation data along strike from the Bremner shear zone of Pavlis and Sisson (2003). The average strikes of foliations (S3) and trends of lineations (L3) are $\sim 300^\circ$ and $\sim 120^\circ$ respectively where the average strikes of foliations (S2) and lineations (L2) associated with the fan surrounding these data and in other parts of the fan are $\sim 280^\circ$ and $\sim 100^\circ$ respectively (Fig. 2 and 6b).

Upper Bremner River section

Observations in this area were made from four camps. Two camps were located north of the Stuart Creek fault (Appendix B: map D and E) and two camps south of the fault (Appendix B: map E and F).

While mapping in the southern two camps we observed the same core zone of the fan defined by steeply dipping S2 cleavage with close to isoclinally folded layering. As with the lower Bremner River section the S2 cleavage rolled out to shallower dips to the north and south (Fig. 5c and 6c). We also found F2 fold geometries showing a decreasing strain gradient comparable to those of the lower Bremner section which were also truncated by the Stuart Creek fault.

Camps north of the Stuart Creek fault also revealed a pattern in decreasing strain gradient. Close to the Stuart Creek fault there were still discernable moderate to shallow dipping S2 cleavages which diverge from layering. At a distance of approximately 10km north of the fault we lost any trace of S2 and only recorded evidence of tight to isoclinal folding of bedding and an associated crenulation cleavage interpreted to be S1. This area also revealed evidence of a more brittle style of deformation with the observation of slickenslides in many locations.

Petrographic analysis also showed that there was a lack of biotite growth in the rocks of this area revealing a decrease in metamorphic grade moving to the north.

Stuart Creek fault

There is a major topographic lineament cutting across the north of our study area following an east-southeast trend. One helicopter stop along the lineament revealed slickenslides and dextral asymmetries along this lineament. We have also observed that this lineament cuts off the northern section of the Bremner foliation fan juxtaposing it against rocks with a different structural history. Pavlis et al. (2003) observed a similar pattern to the west of our area along the Richardson Highway where this lineament separated rocks with different structural histories. We have named this lineament the Stuart Creek fault.

Interpretation of Field Relationships

Inspection of the maps and cross-sections allows a comparison of our area to a model presented by Teyssier et al. (2002). When our cross-sections (Fig. 5a, b, and c) were compared to Teyssier et al.'s (2002) model (Fig. 4) a distinct similarity in the foliation geometries were observed. O'Driscoll et al. (2006) tried to create a modified version of Teyssier et al.'s (2002) model to match deformation observed in the Bremner foliation fan. O'Driscoll (2006) recognized that although Teyssier et al.'s (2002) model could reproduce the geometry of the fan, it failed to predict both finite strain variation and lineation trends. By inverting the geometric variables of the model, placing a zone of distributed shear above a zone of strain localized shear, he was able to produce a foliation pattern that matched both the observed geometry and finite strain pattern.

Rocks within the brittle-ductile transition zone showing a similar foliation pattern to the one we have observed have been described as an attachment zone by Teyssier et al. (2002) (Fig.

4) or a decoupling horizon by Pavlis and Sisson (2003). After comparison of our observed structure and these models I conclude that the rocks of the Bremner Foliation Fan are representative of this attachment zone or decoupling horizon and show how strain is recorded in rocks within the brittle-ductile transition up dip from a strike-slip shear zone.

Interpretation of the Bremner shear zone and the Stuart Creek fault

Structural observations made in the lower Bremner River section have lead me to the interpretation that the Bremner shear zone of Pavlis and Sisson (2003) is a younger and separate structure from the Bremner foliation fan described above. The grouping of poles of foliations in figure 6b shows what I interpret as two separate groupings of foliation poles, and our mapping corroborates this interpretation, where the second group of foliations can be seen to cut across the foliation fan along strike from the Bremner shear zone of Pavlis and Sisson (2003). Vertical cleavages (S3) of the Bremner shear zone were also observed to cross cut and even fold the moderately dipping cleavages (S2) of the fan (observations from this study and Pavlis and Sisson, 2003). From this I conclude that the Bremner shear zone of Pavlis and Sisson (2003) and possibly the Wernicke shear zone are younger D3 structures.

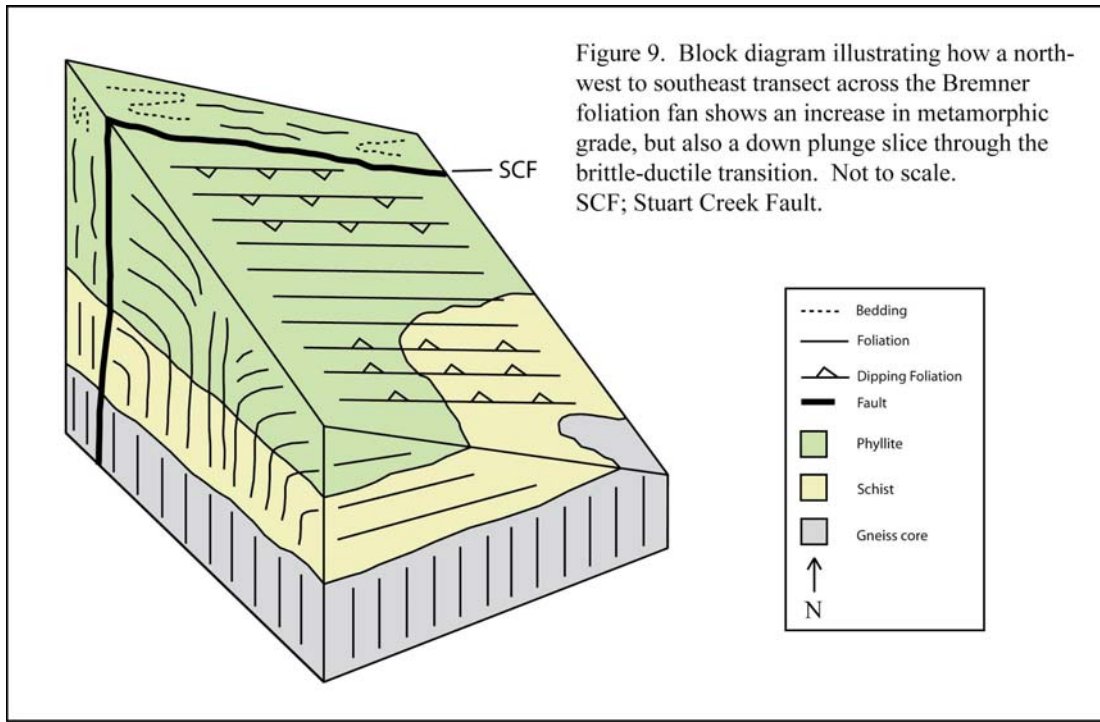
Recognition of the Bremner foliation fan leads to an alternative hypothesis for the association of the Stuart Creek fault with the western termination of the CMC. While the Stuart Creek fault was initially thought to be a part of the deformation events associated with the CMC, it now appears that it is a younger brittle fault and not associated directly with the Bremner foliation fan. Distinct structural histories as well as Petrographic analyses of samples north and south of the Stuart Creek fault (see above) illustrate this interpretation.

Samples; 04ALO24b, 04ALO25a, 04ALO30, and 04APa04 show a conspicuous absence of biotite, yet all samples south of the Stuart Creek fault contain greenschist facies or higher

grade assemblages with ubiquitous biotite (Appendix A). 04ALO30 and 04APa04 clearly show pressure solution textures where 04ALO24b and 04ALO25a, further to the north, show pressure solution associated with micro-cracking and veining in the rock (Appendix A). This could be associated with the fact that 04ALO30 sits in a valley 400-500 vertical feet below 04ALO24b and 04ALO25a, and that 04APa04 is ~7 km away from the three other samples, but is more likely a result of the rheological difference between metapelite and more quartz rich metagraywack rocks (Fig. 2). The geographically closest samples to the south-southwest, samples 03APa81 and 03APa111, show distinctly higher levels of pressure solution deformation and evidence of biotite growth (Appendix A and Fig. 2). Samples with the closest textures to 04ALO24b, 04ALO25a, 04ALO30, and 04APa04 are samples on the northwestern limit of the Bremner Foliation Fan area; samples 04ALO126 and 04ALO129 (Appendix A and Fig. 2). If samples 04ALO24b, 04ALO25a, 04ALO30, and 04APa04 were originally associated with the samples of the northwestern portion of figure 2, samples 04ALO126 and 04ALO129, it would indicate that the Stuart Creek Fault would have to be a younger strike slip event than the Bremner foliation fan and the displacement indicated by this correlation is 70-90km of dextral offset.

This makes sense when one compares this with the work of Pavlis et al. (2003). Our lower grade samples in this area would replace their “Domain 2” rocks putting rocks of similar texture and metamorphic grade adjacent to one another. This then allows the extension of the Bremner foliation fan into the “Domain 1” rocks of Pavlis et al. (2003) that show “a single constrictional strain event associated with the ductile section of a dextral strike slip fault.” The “Domain 1” rocks are along strike from the core of the Bremner foliation fan and extending the

fan into the area of Pavlis et al. (2003) creates a thicker crustal column extending through the brittle-ductile transition zone (Fig. 9).

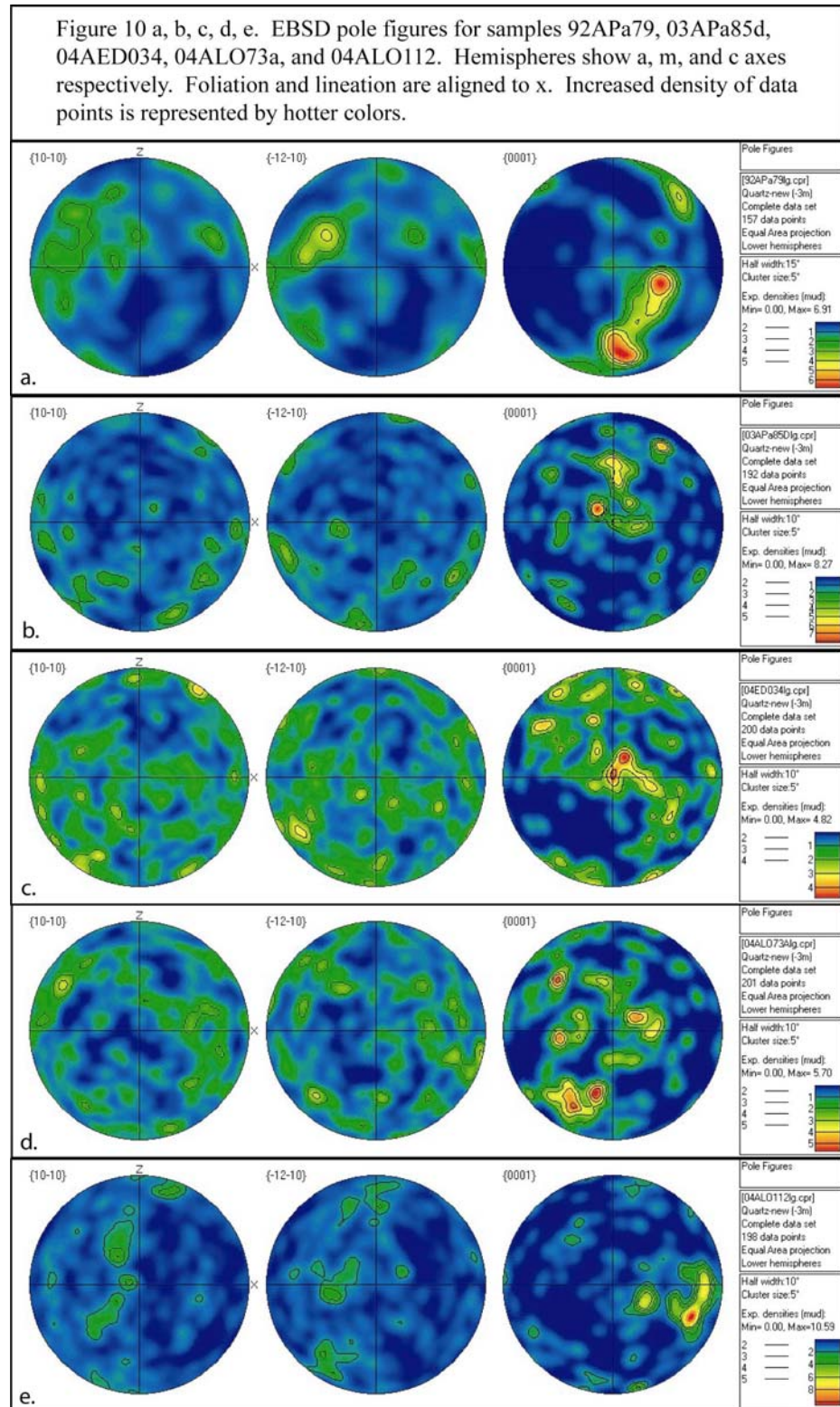


EBSD RESULTS

Electron Back Scatter Diffraction (EBSD) was used to determine c-axis preferred orientations of quartz crystals in samples from the CMC and to use this lattice preferred orientation (LPO) to infer a strain history, particularly information on sense of shear. Samples were collected through a range of metamorphic conditions, and across the Bremner foliation fan with intent to use the quartz fabrics to evaluate shear sense variations across the fan. We preferentially sampled quartz veins that had been clearly deformed, primarily as boudinaged veins along the principal S2 foliation.

The results of this study were surprising in that no LPO of quartz grains was observed in the majority of the samples. The data for samples 92APa79, 03APa85d, 04AED034, 04ALO73a,

and 04ALO112 are shown in figure 10 (a, b, c, d, and e respectively) as stereographic projection pole figures.



The a, m, and c axes are shown respectively in the three plots from left to right. The x axis (east to west) in the plots represents the vertical foliation plane with the lineation also aligned east to west and horizontal along this plane. Increasing density of c-axis data groupings is represented by increasing warmth of colors in the plots. If there were enough strain to create an LPO, under pure shear the c-axes data groups should align themselves toward parallelism with the maximum finite shortening axis (pole to foliation) which when plotted creates a pattern of higher density localizations represented by “hot” colors at the top and bottom of the sphere (Schmid and Casey, 1986). Under simple shear the c-axes should form a girdle along the z axis of the plot (north to south) with maxima at the top and bottom creating a vertical band of “warmer” colors (Schmid and Casey, 1986).

In the case of samples 03APa85d, 04AED034, and 04ALO73a the c-axes data groupings are shown as the green masses covering the plot area (Fig. 12 b, c, d) with no distinctive clustering or development of a girdle. Thus in those samples quartz is nearly randomly oriented and has not been significantly realigned by deformation. C-axes in sample 04ALO112 show an interesting pattern where the c-axes have aligned to the lineation, parallel with the foliation (Fig 12e). This type of alignment is unlike any pattern typically modeled in computer simulations of LPO's created by dynamic recrystallization (Twiss and Moore, 1992). The observed pattern may be an effect of strain superposition as this sample was collected along strike from the core zone of the Bremner shear zone of Pavlis and Sisson (2003) (Fig. 2), though the general geometries of the two structures are so similar this is unlikely. Cox and Etheridge (1983) showed that preferred orientation can develop in response to oriented growth mechanisms during crack-seal deformation. As a boudin is stretched parallel to foliation, a crack is formed perpendicular to the foliation. Quartz fibers grow by preferential rejoining at each crack-seal growth increment with

those grains having fast growth directions parallel to the displacement vector, which in our case is parallel to the foliation (Cox and Etheridge, 1883). After observation of quartz fibers parallel to the foliation in this sample, I would argue that this was the style of deformation occurring in sample 04ALO112, and resulted in the c-axes of our sample developing parallel to the foliation.

Sample 92APA79 produced a plot closest to a typical c-axis girdle when compared to published literature (Fig. 12a) (Schmid and Casey, 1986). However, if this is the case the cut of the slide was $\sim 40^\circ$ off from its proper orientation, and the data needs to be rotated back that amount to show any evidence of an LPO or shear sense. The LPO in sample 92APA79 is not surprising despite the lack of an LPO in the other samples because this sample was collected in upper amphibolite facies schists near the gneissic core of the CMC (Fig. 2). Thus, this sample was deformed under much higher temperature conditions, where crystal plasticity should be more prominent relative to samples 92APA79, 04ALO73a, and 04AED034, which were collected from much lower grade rocks.

In retrospect, the absence of a strong LPO in these deformed veins is not necessarily anomalous. One possibility for the absence of an LPO is that quartz crystals annealed by post-tectonic heating. That is, static recrystallization of a quartz rich rock might erase any LPO that dynamic recrystallization may have created. This thought has largely been abandoned, however, because a study performed by Heilbronner and Tullis (2002) showed that static annealing of quartzites did not affect the LPO of a rock. The annealing did change the crystal size within the samples, but the LPO was retained (Heilbronner and Tullis, 2002). In addition, statically recrystallized rocks typically show clear evidence of this overprint in the form of grain growth and random mineral growth splays; textures that have not been observed in the CMC except in rocks within contact aureoles of large plutons (Sisson et al., 1989). With this in mind it seems

clear there was another reason for the lack of an LPO in our samples. The most important observation constraining an interpretation is that all of the samples were collected from veins that were boudinaged. Boudinage only occurs when the boudinaged rock has markedly higher viscosity than the enclosing matrix (Smith, 1975; Smith, 1977), and because of this relationship, boudinage can produce relatively low finite strain in the boudin material when the matrix undergoes very large finite strain. Thus, the lack of an LPO in the veins implies the boudinage occurred with little, if any, flow within the veins themselves, and deformation was primarily accommodated by boudin necking or as with sample 04ALO112 crack-seal deformation.

With this in mind attempts were made using EBSD to sample the LPO in the matrix around the veins and boudins. Unfortunately, even after further polishing, the matrix grains still did not receive sufficient polish as a result of the sample roughness created from a difference in strength of larger grained quartz versus that of the microcrystalline micaceous matrix. The result of having no polish on the matrix grains was that there were no discernable c-axis patterns from individual grains. The absence of significant LPO in these quartz veins has important implications for the bulk rheological behavior of these materials as boudins and stretched grains are usually associated with crystal plastic deformation within the Brittle-ductile transition (Raymond, 2002). Thus, as a second part of this study I conducted a detailed petrographic micro-textural analysis of our samples to identify any variations in deformation mechanisms that could lead to this anomalous behavior in our samples.

PETROGRAPHIC ANALYSIS

Observations made at the microscopic scale show evidence that the rocks of the Bremner foliation fan were deformed under dextral shear. Samples were observed on a plane perpendicular to foliation and parallel to lineation, the movement plane assuming simple shear, in order to observe any grain shape asymmetries from deformation. In all of our thin sections the

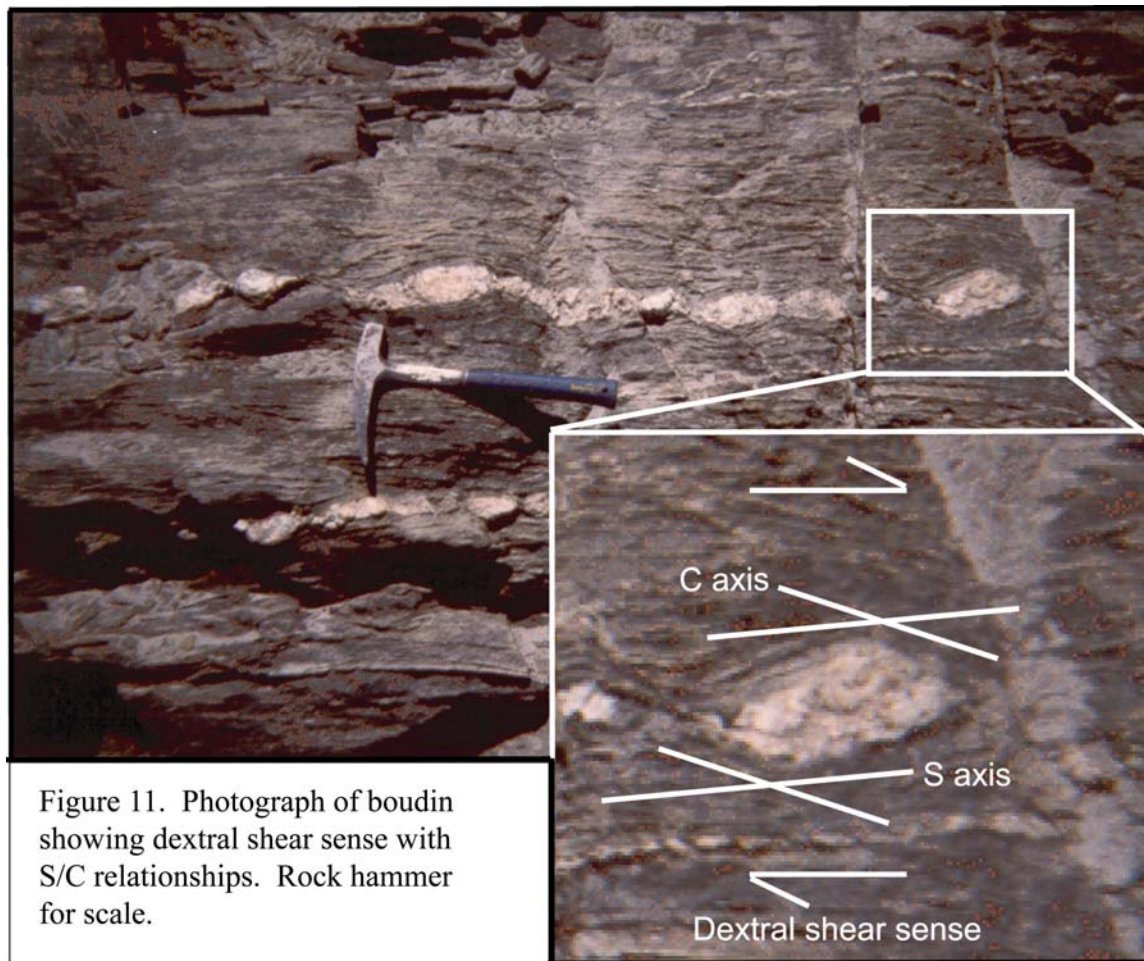
majority of grains counted, an average of ~65 %± total grains counted per sample, showed no clear asymmetries indicative of shear sense. Nonetheless, all but one of the samples had the majority of the remaining grains show dextral asymmetries, with an average of ~21 %± total grains counted per sample (Table 2 and Fig. 2). Observations made on outcrops and sigmoidal shaped grains and boudins provide further evidence of dextral shear (Fig. 11). When plotted on the map (Figure 2) the samples show a subtle increase in percentage of dextral grains counted sampling from the northwest to the southeast. Samples in the NW show an average of 10 to 20 % of grains counted with dextral asymmetry while samples to the SE showed an average of 30-40% dextral grains (Fig. 2). The difference is subtle; however it also coincides with an increase in temperature, as the metamorphic grade increases from greenschist to upper amphibolite facies in the same direction (Fig. 9).

Table 2. Shows number of grains counted per sample with observed shear sense and percentage of grains per sample showing each observed shear sense. Dark gray highest percentage of grains, light gray intermediate, white low.

Sample	# of grains counted				Percentage of grains/sample		
	sinistral	neutral	dextral	total # of grains	% sinistral	% neutral	% dextral
04AED41	26	35	42	103	25	34	41
04AED57	18	75	19	112	16	66	18
04AED75	25	52	36	113	22	46	32
04ALO24b	1	130	10	141	1	92	7
04ALO25A	25	82	43	150	17	55	28
04ALO30	45	87	63	195	23	45	32
04ALO84	13	89	33	135	10	66	24
04ALO102	10	101	18	129	8	78	14
04ALO126	27	124	37	188	14	65	21
04ALO129	30	92	29	151	20	61	19
04APA4	35	117	62	214	16	55	29
03APa2	24	125	40	189	13	66	21
03APa81	34	124	47	205	17	60	23
03APa97	32	111	36	179	18	62	20
03APa111	17	90	33	140	12	64	24

The metamorphic grade of the area, shear evidence observed in thin sections, and the pattern of developing LPOs, all increase along a northwesterly trend across the foliation fan (Fig.

2, 9). These samples indicate that there is a qualitative correspondence between metamorphic grade and development of clear dislocation creep microstructures. Samples deformed under amphibolite facies conditions, south of the Bremner River, predominantly show dislocation creep microstructures suggesting this, as does the observation of pressure solution in lower grade rocks to the north (Figure 2). There are however exceptions to this generalization and it seems clear that other factors must be influencing the development of different deformation mechanisms.



DISCUSSION

Dislocation Creep in the CMC

Hirth and Tullis (1992) defined three different regimes of dislocation creep in quartz aggregates; regime 1--grain boundary migration (GBM) between deforming crystals; regime 2--

deformation can be observed as progressive sub-grain rotation resulting in core and mantle structures; and regime 3--both deformation mechanisms occur creating core-mantle structures with sub-grains that are larger than those in regime two.

The textures of regimes two and three create an LPO of the type that were anticipated in our initial EBSD work. More detailed petrographic analysis revealed why these anticipated LPO's were absent. First, the quartz grains in our samples did not seem to have undergone enough strain to have created an LPO. There is evidence of crystal plastic deformation in our samples; the majority of them show irregular grain boundaries and undulatory extinctions evidence of grain boundary migration (See Appendix A; samples 03APa02, 03APa97, 04AED41, 04AED57, 04AED75, 04ALO84, 04ALO102, 04ALO126, 04ALO129). This would put the rocks of the CMC in the first deformation regime of Hirth and Tullis (1992), which explains why there was no LPO observed in our samples. Quartz rocks within this regime do not form an LPO until they have reached a microstructural steady state and been fully (100%) recrystallized. In experiments this full recrystallization was only observed in samples of fine grained novaculite which were quickly recrystallized through GBM (Hirth and Tullis, 1992). Our samples, composed of 10-65% quartz are nowhere near the composition of a fine grained pure novaculite and would require much more deformation to show the same result through GBM

Stipp et al. (2002) produced a strain rate vs. temperature diagram where natural samples from the Tonale Line and the Ruby Gap Duplex were compared to the experimental samples of Hirth and Tullis (1992) (Fig. 12). Micro-textural observations, made by Stipp et al. (2002), are bulging recrystallization (BLG), subgrain rotation recrystallization (SGR), and grain boundary migration recrystallization (GBM). Field samples were plotted using previously established flow

law equations and micro-textural observations, only water added samples were used from Hirth and Tullis (1992) (Stipp et al., 2002). The BLG, SGR, and GBM described by Stipp et al. (2002) compare to the 1st, 2nd, and 3rd deformation regimes of Hirth and Tullis (1992) respectively, and are separated by dashed lines in Figure 12.

I calculated rudimentary strain rates for the samples of the fan. First an X/Z strain end member of 45 and a longitudinal strain (ϵ) of 9 were calculated from data collected by Pavlis and Sisson (2003). Pavlis and Sisson (1995) state that deformation of the CMC took place over approximately 8 my. Sisson et al. (2003) state that early syn-deformational intrusives have U-Pb and ⁴⁰AR-³⁹AR ages of ~54ma, and Sisson et al. (1989) used ⁴⁰AR-³⁹AR dating on biotite to show that the CMC cooled rapidly from 52-50ma. From this information I calculated approximate strain rates using the strain data and three periods of deformation; 8my, 4my, and 2my. From those data strain rates for the fan ranged from 7.1×10^{-13} -s to 3.5×10^{-14} -s. When the range of these strain rates, with the range of metamorphic temperatures of the fan is plotted on Figure 12 we see that our samples should be located in the 3rd deformation regime of Hirth and Tullis (1992). These observations lead us to ask the question, “Why did the rocks of the CMC produce little to no evidence of forming an LPO even when observations on metamorphic conditions and strain rates indicate they have been deformed under the necessary field conditions to create an LPO?”

The Importance of Rheology

With the exception of pure quartz veins, of all the samples that I examined from the CMC, none had more than 65 percent quartz in it. This is a result of their greywacke and argillite protoliths deposited as late Cretaceous turbidite flows (Hudson and Plafker, 1982, Plafker et al., 1994). This also explains the high amount of feldspars and phyllosilicates

throughout the CMC samples as the source to those flows is thought to be from metaplutonic complexes in Southeastern Alaska and British Columbia (Plafker et al., 1994). These mineral assemblages of the CMC are important to the deformation processes which have been observed.

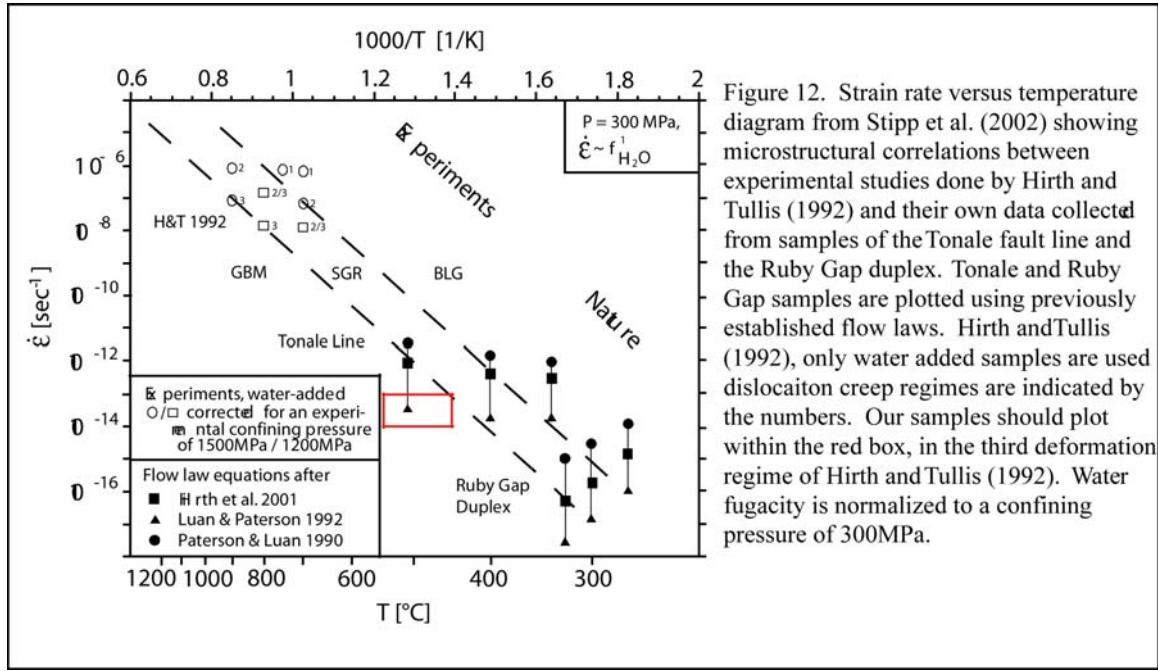


Figure 12. Strain rate versus temperature diagram from Stipp et al. (2002) showing microstructural correlations between experimental studies done by Hirth and Tullis (1992) and their own data collected from samples of the Tonale fault line and the Ruby Gap duplex. Tonale and Ruby Gap samples are plotted using previously established flow laws. Hirth and Tullis (1992), only water added samples are used dislocation creep regimes are indicated by the numbers. Our samples should plot within the red box, in the third deformation regime of Hirth and Tullis (1992). Water fugacity is normalized to a confining pressure of 300MPa.

Metamorphic grade clearly increases across the area from the northwest to the southeast, and this temperature variation may have influenced and increased the number of grains recording dextral shear along the same transect (Fig. 2). Figure 2 also shows the dominant deformation mechanism observed in each sample; pressure solution or dynamic recrystallization. It was qualitatively observed in the field that metagraywackes recorded a shape fabric (finite strain fabric) and metapelites showed classic fabric superposition textures (S1-S2 overprints, etc.). The initial interpretation of this was that the metagraywackes were deforming by penetrative flow, presumably crystal plasticity or grain boundary sliding and the metapelites were deforming by some kind of pressure solution mechanism to make the overprinted foliations.

Both deformation mechanisms occur in many of our samples. Some seem to show evidence of pressure solution followed by dynamic recrystallization (04ALO126) and others

seem to show the opposite sequence (04APA97) (Appendix: A). Observations in sample 04ALO102, which is a stretched pebble conglomerate that includes argillite rip up clasts, provide what is potentially the most important “smoking gun” to explain the behavior in these rocks. Specifically, evidence for both deformation mechanisms were observed in the sample but were lithologically controlled (Appendix: A) dynamic recrystallization occurred readily in the quartz sands and pebbles, and pressure solution dominating in the rip up clasts (Appendix: A). That is the argillite pebbles “snake” their way through the rest of the rock suggesting pressure solution within the argillite pebble while the matrix flowed by crystal plasticity. After a review of the rest of our samples it was noted that pressure solution was seen more clearly in metapelite samples and dynamic recrystallization was observed in the more quartz rich metagraywacke samples. The two types of rock each show both deformation mechanisms but the metapelite samples seemed more susceptible to pressure solution and metagraywacke showed more evidence of GBM.

It could easily be argued that the observed pattern resulted from an overlapping of deformation mechanisms created as the rocks traveled through the different deformation regimes. However, I argue that this area of the CMC is a nearly perfect field laboratory for the observation of the gradational change from pressure solution to a more pure crystal plastic form of deformation as would be observed deeper in the gneissic core because the thermal history is relatively simple.

This deformation mechanism distribution is interpreted to be an effect of hydrous rocks undergoing temperatures and conditions which are conducive to both types of deformation. As previously stated, the rocks in this area have been observed to have been deformed under maximum temperatures and pressures of $\sim 650^{\circ}\text{C}$ and $\sim 4\text{kb}$ respectively, well within the range of

natural crystal plastic deformation. According to the strain rate versus temperature diagram created by Stipp et al. (2002) our samples should be in the 3rd deformation regime of Hirth and Tullis (1992), while our observations show that they have barely reached the 1st deformation regime of Hirth and Tullis (1992) (Fig. 12). These observations lead to the following discussion of why the rocks of the foliation fan do not show evidence of higher deformation regimes.

Explanations for Observed Deformation

One explanation for our rocks showing little evidence of crystal plastic deformation is the confining pressure. Hara and Nishimura (1977) stated that the minimum pressure for dislocation creep in schists is 5-7kb. Tullis and Yund (1989) established that quartz in the lab at confining pressures <5.5kb even in the presence of water would still deform brittly. With our pressures of 4kb or less it could be argued that we did not achieve the base confining pressure of 5kb and this is why our rocks show little evidence of dynamic recrystallization. However, the rocks of the CMC have been described as upper green schist to lower amphibolite facies with observations of minerals like garnet, andalusite and sillimanite (Raymond, 2002). The presence of these minerals, together with thermobarometry (Sisson et al. 1989) indicates that the CMC was metamorphosed at pressures of less than 350MPa and temperatures of 450-650°C. Our samples were most likely deformed at temperatures of 450°C or less, but they have still reached temperatures equal to, to ~ 200°C above the lower bound observed for dislocation creep in naturally deformed rocks. Hirth and Tullis (1992) increased the deformation regimes of their samples by increasing temperature and or reducing the strain rate. Therefore, one might think that there should be evidence of higher deformation regimes within CMC with the observed high temperature metamorphism.

One additional consideration is the role of water. Weinberger and Sisson (2003) show that the rocks of the CMC are filled with fluid inclusions showing pressures and temperatures lower than the peak metamorphic temperatures. Moreover, quartz veins are ubiquitous in the CMC, particularly at lower grade, implying large-scale mobility of water (Sisson and Hollister, 1988). Indeed Bowman et al. (2003) shows large-scale metasomatic effects from water influx to the complex. An important point also is that these studies argue that the fluids involved are extensively traveled. In fact Weinberger and Sisson (2003) make the argument that some of the fluids involved in the deformation of the CMC may have traveled up to 100km. This means that the rocks of the CMC were water saturated and mobility of fluids was not the exception. Here I suggest that this water may have played a major role. I suggest the hypothesis that the phyllosilicate rich rocks of the CMC have hindered dynamic recrystallization and potentially promoted pressure solution in the CMC where a more pure quartz rock would have undergone higher regimes of crystal plastic deformation and potentially formed a LPO.

Pore Space

Gundersen et al. (2002) created a model showing the effects of phyllosilicates associated with quartz sandstones undergoing pressure solution. While their model referred to pressure solution compaction of sands, parts of their model may be applicable. Renard et al. (2001) suggest that phyllosilicates speed up pressure solution within sands by a mechanical effect where the transport properties of the contacts are enhanced, either due to an increased thickness of the water film at the contacts or equivalently an increase in the diffusion constant at the grain contact. However, sandstone is a pore-space-rich environment, quite different from a phyllite or schist like those of the CMC. In samples where pore space was limited Gundersen et al. (2002) saw that the mobility of fluids was greatly increased. Higher fluid mobility was attributed to the

lack of precipitation locations within the rocks. This concept agrees with the observations made by Weinberger and Sisson (2003) where fluids were well traveled. In fact this lack of intergranular pore space and resulting fluid mobility could contribute to fluid:rock ratios of 4:1 to 1.5:1 suspected by Sisson and Hollister (1988) as a heating element for the CMC. The resultant high fluid:rock ratios could also contribute to fluid pressures necessary to induce hydrofracture resulting to the large amounts of quartz veining within the CMC.

The Importance of aluminum

Aluminum rich minerals are present throughout the CMC, ranging from sheet silicates like muscovite, biotite, and chlorite, to orthosilicates like garnet to aluminum silicates like andalusite and sillimanite (Hudson and Plafker, 1982; Sisson and Hollister, 1988; Sisson et al., 1989; Plafker et al., 1994; Pavlis and Sisson, 1995). We even see in sample 04ALO102 chlorite surrounded by biotite (Appendix: A), while this may be evidence of a retrograde reaction it does tell us that the rocks of the CMC have the elements necessary to form both minerals and this reaction is consistent with pressures and temperatures in the area (Sisson and Hollister, 1988; Sisson et al., 1989). This mineral assemblage and the presence of quartz + andalusite ± sillimanite veins makes it easy to assume that there was plenty of free aluminum in the fluid system of the CMC (Pavlis and Sisson, 1995; Bowman et al., 2003).

It is accepted that small amounts of Al^{3+} and Fe^{3+} plus appropriate amounts of Na^+ , Li^+ , K^+ , and or H^+ will substitute for silica within the quartz crystal lattice (Nesse, 2000). Niemeijer and Spears (2002) observed that pressure solution compaction rates were decreased in a mica and quartz mixture deformed at a temperature of 500°C and a pressure of 1kb. Niemeijer and Spears (2002) report that in geochemical literature the presence of Al^{3+} in solution is expected to decrease silica solubility, precipitation rates and dissolution rates, but they also make the

disclaimer that experiments have to be done where diffusion or precipitation are the rate controlling conditions. Their data does support their statement as the amount of muscovite in their experiments was too little to create a load-supporting framework or matrix. With the large amounts of aluminum in the fluids of the CMC it is possible that aluminum ions became associated with imperfections in the crystal lattice formed at micro-cracks along the edges of quartz grains previously created by brittle deformation during subduction. Just as with the work of Niemeijer and Spears (2002) this association between aluminum and quartz would decrease silica solubility, precipitation rates and dissolution rates of quartz in the CMC. A lack of precipitation sites for silica in solution could prevent the formation of sigma shaped quartz grains and explain why an average of 60% of quartz grains counted per slide did not show evidence of a shear sense.

In samples 03APa2, 03APa97, 03APa111, 04ALO126 quartz grains and quartz rich zones were observed where a rind of biotite has formed around the quartz (Appendix: A). In sample 04ALO126 the whole grain has not been surrounded but the biotite has grown in an imperfection in a round grain. The aluminum associated with imperfections and microcracks along the outer edges of quartz grains could also promote the growth of biotite or other phyllosilicates along the edges of quartz crystals and or quartz rich zones. The growth of this biotite could then further reduce pore space and or silica precipitation locations, reducing the effects of pressure solution on quartz grains and promoting it in the phyllosilicate rich matrix. This lack of precipitation sites for silica in solution could prevent the formation of sigma shaped quartz grains and explain why an average of 60% of quartz grains counted per sample did not show evidence of a shear sense.

The use of the aluminum ions associated with the quartz crystal lattice in biotite growth could potentially remove hydrogen ions already associated with the quartz, or it could leave behind an associated hydrogen ion in the quartz crystal lattice imperfection. This addition or removal of hydrogen from quartz is important because it has been assumed that diffusion of inclusions (especially water) in quartz crystals is linked to the creep of the quartz lattice in dynamic recrystallization, the specific species of water (H^+ , OH^- , H_2O , H_3O^+) that is associated with lattice motions (dislocation creep) has not been determined (Blacic, 1981; Kronenberg and Tullis, 1984; Linker et al., 1984; Post and Tullis, 1998). This could mean that emplacing or removing hydrogen into the outer rim of the quartz crystal lattice is less significant than described above. However, it has been generally accepted that free hydrogen is the water defect that speeds up the movement of dislocations in the crystal lattice in olivine, thus it would not be too hard to accept that free hydrogen may have a similar effect in quartz (Justice et al., 1982; Mackwell and Kohlstedt, 1990; Chen et al., 1998; Brodholt and Refson, 2000). Reducing the amount of hydrogen associated with quartz crystals could hinder dynamic recrystallization, possibly explaining why the quartz crystals we observed only reached the first deformation regime of Hirth and Tullis (1992). In contrast, the addition of hydrogen to the lattice could be an important step toward the switch to crystal plastic deformation in quartz grains as temperature and pressure increase with depth, the beginning of which is represented in the southeast of the fan by greater amounts of GBM in samples. Clearly, more studies are needed on the effects of phyllosilicates in the presence of quartz under the conditions of the brittle-ductile transition before this hypothesis can be thoroughly examined.

Effects of Increased Pressure Solution

The previous sections describe how pressure solution could be promoted in phyllosilicate rich rocks under brittle-ductile transition conditions. The rocks of the CMC are very rich in micas and other clay minerals, ranging from 35-90% phyllosilicates. Unlike the experiments carried out by Niemeijer and Spears (2002) the rocks of the CMC contain enough phyllosilicates to create a load-bearing framework. The observed growth of biotites around quartz grains further supports this conclusion. The increased pressure solution caused by high fluid mobility, a lack of pore space, and high levels of free aluminum along with this load-bearing framework would create a situation where the majority of the strain in the CMC would be taken up by pressure solution in the phyllosilicates. This would further reduce the amount of strain taken up by quartz within the deformational system in the CMC, adding to the reasons for a lack of an LPO or evidence of higher levels of dynamic recrystallization in the rocks of the Bremner foliation fan.

As far as the evolution of deformation mechanisms across the brittle-ductile transition this ease of phyllosilicate mobility becomes important. Where a micaceous load bearing framework would be missing in more quartz rich metagraywacke within the CMC, the growth of biotites and highly mobile phyllosilicates could be evidence of the transition toward creating one. As this motion of phyllosilicates continues separation into mica rich and quartz rich layers could ensue. The rocks of the Bremner foliation fan may be showing us evidence of the evolution of rocks through the brittle-ductile transition changing into basement gneissic rocks. In fact, the western termination of the CMC may be a perfect field laboratory for studying the evolution of deformation mechanisms and their interactions with different metamorphic rock facies with respect to rheology, strain rate, pressure, and temperature changes.

One important point to remember with respect to this study and others are the effects of scale. Microtextural and hand-sample scale observations are used as analogues to understand large scale deformation. While this is a well accepted and widely used technique, the understanding of large scale regional deformation may be hindered by focusing on the smaller scale observations. This is because large scale regional deformation takes place as a conglomeration of multiple smaller scale deformation mechanisms and events. For this reason many more small scale and large scale studies need to be carried out across the CMC to ensure a complete understanding of the deformational processes and events that created it.

SUMMARY AND CONCLUSIONS

Analysis of new structural data along the western termination of the CMC has revealed the existence of a D2 foliation fan, referred to here as the Bremner foliation fan. This structure is thought to be the exposure of a foliation pattern created up dip (structurally above) from a dextral strike slip shear zone resulting from oblique subduction along the Alaskan-Aleutian Arc in the early Eocene. Modeling suggests that this structure is the result of changing finite strain below the centers of moving blocks of brittle crust (Teyssier et al., 2002; Pavlis and Sisson, 2003; O’driscoll, 2006), but the foliation fan developed during the prograde metamorphism (D2) and does not fit the general “attachment” model of Teyssier et al., (2002). Instead, the system appears to have been driven from below by a shear zone at depth that passed upward into the cleavage fan (O’Driscoll, 2006). Shear sense indicators, although generally weak, recognized in this study indicate dextral shear through the cleavage fan, which supports O’Driscoll’s (2006) interpretation of the complex but is inconsistent with a hypothesis that the cleavage fan is a “cusp” beneath upper crustal rigid blocks.

Field observations together with textural observations in samples provide new insights into the structural history of the western termination of the CMC. Field observations indicate

that the Stuart Creek shear zone of Pavlis et al. (2003) is a younger, brittle fault that is not directly related to the Bremner foliation fan. This fault has displaced rocks deformed by the fan approximately 90km in a dextral sense. It has also been determined that the Bremner shear zone of Pavlis and Sisson (2003) and possibly the Wernicke shear zone are younger (D3) shear systems that cross cut and merge with the Bremner foliation fan.

EBSD studies indicate little to no evidence of a LPO developing in the deformed quartz veins other than a sample from boudinaged quartz vein in high-grade schists near the gneiss transition. This result was interesting in that the rocks of the CMC had undergone pressure and temperature conditions where the dynamic recrystallization necessary to create an LPO was expected to have occurred. The sampling of boudinaged quartz veins could have played a factor in this observation because they may have behaved as rigid bodies during boudiniazation with little dynamic recrystallization.

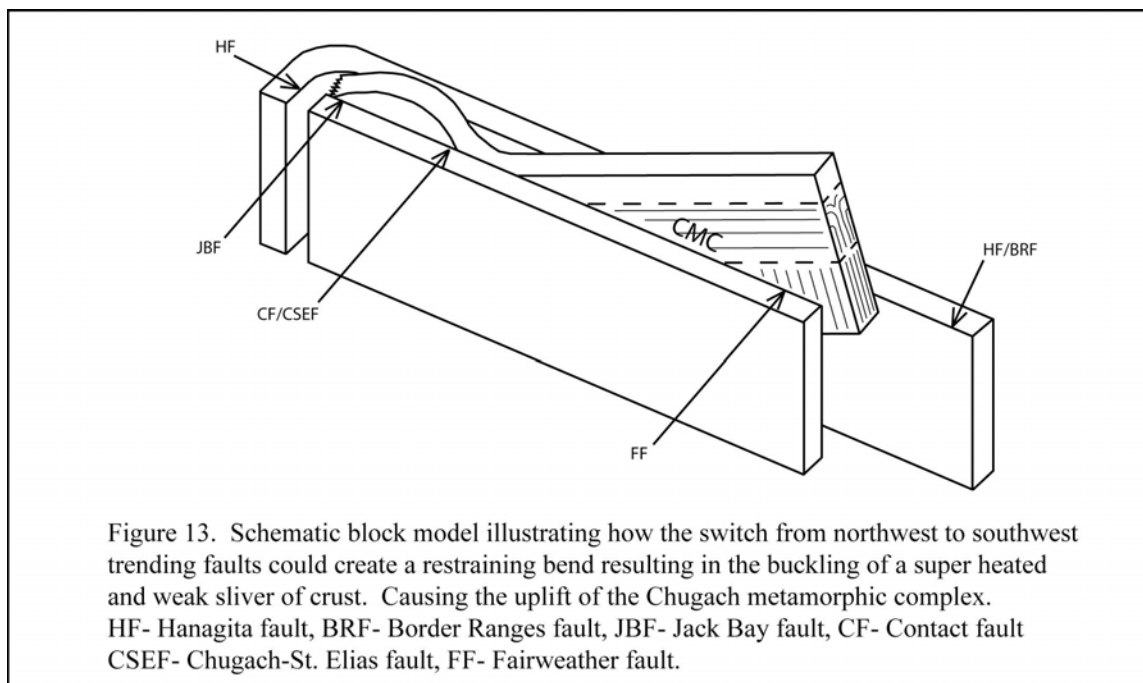
Microstructural observation suggests that this hypothesis is an oversimplification, however, and that several factors may have contributed to the lack of development of an LPO in the samples. First, the matrix materials show clear evidence of mixed behavior, with both pressure solution and crystal plastic mechanisms present. This mixed behavior, however, is strongly compositionally dependent with crystal plastic textures strongly developed in metagraywacke and pressure solution dominant in metapelites. This conclusion is important because it provides a simple explanation for the observation that the metagraywacke typically show a finite strain fabric whereas the metapelites show superposed mica foliations. Second, increasing metamorphic grade produced a spatial variation in deformation mechanism, but this effect is secondary compared to compositional distinctions. Finally, other effects also probably played a role, including increased pressure solution caused by high fluid mobility, a lack of pore

space, high levels of free aluminum, and a load-bearing framework of phyllosilicates. However, more work is needed to thoroughly examine the roles of these processes in producing the observed microstructural variations and the effects they may have on models of mid-crustal deformation (Bos and Spiers, 2001; Bos et al., 2000; Stunitz and Fitz Gerald, 1993; Walniuk and Morris; 1985).

FUTURE WORK

The discovery of the Bremner foliation fan opens up many avenues for future work in the CMC. The first of which is how far east and west can the fan be mapped? We have hypothesized the foliation fan could be extended into the field area of Pavlis et al. (2003), but that area and areas further west should be mapped in more detail to test the theory. Mapping the fan to the east is particularly important because we are not sure if the Bremner foliation fan extends down dip into a homogeneously deformed gneissic zone as predicted by models (Teyssier et al., 2002; Pavlis and Sisson, 2003; O'Driscoll, 2006) (Fig. 4).

The mechanism by which the CMC has been uplifted is another important set of studies that need to be carried out in the future. My hypothesis here is that rocks north of the Stuart Creek Fault have been moved almost 90 km relative to the south. This combined with the description of a back thrusting event to the north west of the CMC made by Pavlis et al. (2003) lead to the idea that the uplift of the CMC could be from a buckling of the crust. As the rocks of the CMC were transported to the northwest they eventually hit the point where the majority of faults in Alaska bend to the southwest (eg. Fig. 1). The resulting convergence of crust blocks could have produced the back thrusting observed by Pavlis et al. (2003) and produced a buckling of the hot weak block of the CMC resulting in its uplift (Fig. 13).



Future work also needs to be focused on the interactions of phyllosilicates within the deforming crust and especially across the brittle-ductile transition. I have shown here that the effect of phyllosilicates in rocks where crystal plastic deformation was assumed to be the dominant deformation mechanism was unexpected. Many of the studies used in this work have been focused on the pressure solution related effects of phyllosilicates on quartz rich rocks at pressures and temperatures conducive to diagenesis. Because of this more studies need to be done with phyllosilicates and quartz under pressures and temperatures representative of the brittle-ductile transition. This is important because it could have major implications for models of the middle to lower crust and our understanding of these locations.

REFERENCES CITED

- Blacic, J. D., 1981, Water diffusion in quartz at high pressure: Tectonic implications: *Geophysical Research Letters*, vol. 8, iss. 7, pp. 721-723.
- Bos, B., Peach, C. J., Spiers, C. J., 2000, Frictional-viscous flow of simulated fault gouge caused by the combined effects of phyllosilicates and pressure solution: *Tectonophysics*, vol. 327, pp. 173-194.
- Bos, B., Spiers, C. J., 2001, Experimental investigation into the microstructural and mechanical evolution of phyllosilicate-bearing fault rock under conditions favoring pressure solution: *Journal of Structural Geology*, vol. 23, pp. 1187-1202.
- Bowman, J. R., Sisson, V. B., Valley, J. W., Pavlis, T. L., 2003, Oxygen isotope constraints on fluid infiltration associated with high-temperature-low-pressure metamorphism (Chugach metamorphic complex) within the Eocene southern Alaska forearc: *Geological Society of America Special Paper 371*, pp. 237-252.
- Brodholt, J. P., Refson, K., 2000, An ab initio study of hydrogen in forsterite and a possible mechanism for hydrolytic weakening: *Journal of Geophysical Research, B, Solid Earth and Planets*, vol. 105, iss. 8, pp. 18,977-18,982.
- Chen, J., Inoue, T., Weidner, D. J., Wu, Y., Vaughan, M. T., 1998, Strength and water weakening of mantle minerals, olivine, wadsleyite, and ringwoodite: *Geophysical Research Letters*, vol. 25, no. 4, pp. 575-578.
- Cox, S. F., Etheridge, M. A., 1983, Crack-seal fibre growth mechanisms and their significance in the development of oriented layer silicate microstructures: *Tectonophysics*, vol. 92, pp. 147-170.
- Gundersen, E., Dysthe, D. K., Renard, F., Bjorlykke, K., Jamtveit, B., 2002, Numerical modeling of pressure solution in sandstone, rate-limiting processes and the effect of clays: *Geological Society, London, Special Publications*, 200, pp. 41-56.
- Hara, I., Nishimura, Y., 1977, Boundary between subbasal I and subbasal II fields of quartz deformation in geological conditions: *Tectonophysics*, vol. 39, iss. 1-3, pp. 273-286.
- Heilbronner, R., Tullis, J., 2002, The effect of static annealing on microstructures and crystallographic preferred orientations of quartzites experimentally deformed in axial compression and shear: *Geological Society, London, Special Publications*, 200, pp. 191-218.
- Hirth, G., Tullis, J., 1992, Dislocation creep regimes in quartz aggregates: *Journal of Structural Geology*, v. 14, No. 2, pp. 145-159.

- Hudson, T, Plafker, G, 1982, Paleogene metamorphism of an accretionary flysch terrane, eastern Gulf of Alaska: Geological Society of America Bulletin, v. 93, pp. 1280-1290.
- Justice, M. G., Graham, E. K., Tressler, R. E., Tsong, I. S. T., 1982, The effect of water on high-temperature deformation in olivine: Geophysical Research Letters, vol. 9, iss. 9, pp. 1005-1008.
- Kronenberg, A.K., Tullis, J., 1984, Flow strengths of quartz aggregates: grain size and pressure effects due to hydrolytic weakening: Journal of Geophysical research, vol. 89, iss. 6, pp. 4281-4297.
- Linker, M. F., Kirby, S. H., Ord, A., Christie, J. M., 1984, Effects of compression direction on the plasticity and rheology of hydrolytically weakened synthetic quartz crystals at atmospheric pressure: Journal of Geophysical Research, vol. 89, iss. 6, pp. 4241-4255.
- Mackwell, S. J., Kohlstedt, D. L., 1990, Diffusion of hydrogen in olivine: Implications for water in the mantle: Journal of Geophysical Research, vol. 95, no. B4, pp. 5079-5088.
- Nesse, W. D., Introduction to Mineralogy, New York: Oxford University Press, 2000.
- Niemeijer, A. R., Spiers, C. J., 2002, Compaction creep of quartz-muscovite mixtures at 500°C: Preliminary results on the influence of muscovite on pressure solution: Geological Society, London, Special Publications, 200, pp. 61-71.
- Nokleberg, W. J., Plafker, G., Lull, J. S., 1989, Structural analysis of the southern Peninsular, southern Wrangellia, and northern Chugach terranes along the Trans-Alaska Crustal Transect, northern Chugach Mountains, Alaska: Journal of Geophysical Research, vol. 94, iss. B4, pp. 4297-4320.
- Pavlis, T. L., Sisson, V. B., 1995, Structural history of the Chugach metamorphic complex in the Tana River region, eastern Alaska: A record of Eocene ridge subduction: Geological Society of America Bulletin, v. 107, no. 11, pp. 1333-1355.
- Pavlis, T. L., Marty, K., Sisson, V. B., 2003, Constrictional flow within the Eocene forearc of southern Alaska: An effect of dextral shear during ridge subduction: Geological Society of America Special Paper 371, pp. 171-190.
- Pavlis, T. L., Sisson, V. B., 2003, Development of a subhorizontal decoupling horizon in a transpressional system, Chugach metamorphic complex, Alaska: Evidence for rheological stratification of the crust: Geological Society of America Special Paper 371, pp. 191-216.
- Post, A., Tullis, J., 1998, The rate of water penetration in experimentally deformed quartzite: Implications for hydrolytic weakening: Tectonophysics, vol. 295, iss. 1-2, pp. 117-137.

- Plafker, G., Moore, J. C., Winkler, G. R., 1994, Geology of the southern Alaska margin, in Plafker, G., and Berg, H. C., eds., *The Geology of Alaska: Boulder, Colorado, Geological Society of America, The Geology of North America, v. G-1*, pp. 389-449.
- Plafker, G., Nokleberg, w. J., Lull, J. S., 1989, Bedrock geology and tectonic evolution of the Wrangellia, Peninsular, and Chugach terranes along the Trans-Alaska Crustal Transect in the Chugach Mountains and southern Copper river basin, Alaska: *Journal of Geophysical Research*, vol. 94, iss. B4, pp. 4255-4295.
- Raymond, L. A., *Petrology: The Study of Igneous, Sedimentary, and Metamorphic Rocks* 2nd ed., New York: McGraw-Hill, 2002.
- Renard, F., Dysthe, D. K., Feder, J., Bjorlykke, K., Jamtveit, B., 2001, Enhanced pressure solution creep rates induced by clay particles: experimental evidence from salt aggregate: *Geophysical Research Letters*, vol. 28, 1295-1298.
- Schmid, S. M., Casey, M., 1986, Complete fabric analysis of some commonly observed quartz c-axis patterns: Mineral and rock deformation; laboratory studies; the Paterson volume, *Geophysical Monograph*, vol. 36, pp. 263-286.
- Sisson, V. B., Hollister, L. S., 1988, Low-pressure facies metamorphism in an accretionary sedimentary prism, southern Alaska: *Geology Boulder*, vol. 16, iss. 4, pp. 358-361.
- Sisson, V. B., Hollister, L. S., Onstott, T. C., 1989, Petrologic and age constraints on the origin of a low-pressure/high-temperature metamorphic complex, southern Alaska: *Journal of Geophysical Research*, vol. 94, iss. B4, pp. 4392-4410.
- Sisson, V. B., Pavlis, T. L., 1993, Geologic consequences of plate reorganization; an example from the Eocene southern Alaska fore arc: *Geology Boulder*, vol. 21, iss. 10, pp. 913-916.
- Sisson, V. B., Poole, A. R., Harris, N. R., Burner, H. C., Pavlis, T. L., Copeland, P., Donelick, R. A., McLelland, W. C., 2003, Geochemical and geochronological constraints for genesis of a tonalite-trondhjemite suite and associated mafic intrusive rocks in the eastern Chugach Mountains, Alaska: A record of ridge-transform subduction: *Geological Society of America Special Paper 371*, pp. 293-326.
- Smith, R. B., 1975, Unified theory of the onset of folding, boudinage, and mullion structure: *Geological Society of America Bulletin*, vol. 86, iss. 11, pp. 1601-1609.
- Smith, R. B., 1977, Formation of folds, boudinage, and mullions in non-Newtonian materials: *Geological Society of America Bulletin*, vol. 88, iss. 2, pp. 312-320.
- Stipp, M., Stunitz, H., Heilbronner, R., Schmid, S. M., 2002, Dynamic recrystallization of quartz: correlation between natural and experimental conditions: *Geological Society, London, Special Publications*, 200, pp. 171-190.

- Stunitz, H., Fitz Gerald, J. D., 1993, Deformation of granitoids at low metamorphic grade. II: Granular flow in albite-rich mylonites: *Tectonophysics*, vol. 221, pp. 299-324.
- Teyssier, C., Tikoff, B., Weber, J., 2002, Attachment between brittle and ductile crust at wrenching plate boundaries, *European Geophysical Union, Stephan Mueller Special Publication*, v. 1, pp. 75-91
- Tikoff, , B., Fossen, H., 1999, Three-dimensional reference deformations and strain facies: *Journal of Structural Geology*, vol. 21, iss. 11, pp. 1497-1512.
- Tullis, J., Yund, R. A., 1989, Hydrolytic weakening of quartz aggregates: The effects of water and pressure on recovery: *Geophysical Research Letters*, vol. 16, iss. 11, pp. 1343-1346.
- Twiss, R. J., Moore, E. M., 1992, *Structural Geology*, Freeman, New York, NY.
- Walniuk, D. M., Morris, A. P., 1985, Quartz deformation mechanisms in metasediments from Prins Karls Forland, Svalbard: *Tectonophysics*, vol. 115, pp. 87-100.
- Weinberger, J., Sisson, J., 2003, Pressure and temperature conditions of brittle-ductile vein emplacement in the greenschist facies, Chugach metamorphic complex, Alaska: Evidence from fluid inclusions: *Geological Society of America Special Paper 371*, pp. 217-235.
- White, S. R., 2001, Textural and microstructural evidence for semi-brittle flow in natural fault rocks with varied mica contents: *International Journal of Earth sciences: Geologische Rundschau*, vol. 90, No. 1, pp. 14-27.

APPENDIX A: Petrographic Sample Descriptions

Brief descriptions of samples observed under petrographic microscope. Includes, sample type, percentage of quartz grains, percentage of quartz grains showing; no, dextral, or sinistral shear sense. Grain counts to determine shear sense data is summed up in Table 2. Also includes a brief summary of the dominant deformation mechanism, other important microtextures, and important minerals.

Table 2. Shows number of grains counted per sample with observed shear sense and percentage of grains per sample showing each observed shear sense. Dark gray highest percentage of grains, light gray intermediate, white low.								
Sample	# of grains counted				Percentage of grains/sample			
	sinistral	neutral	dextral	total # of grains	% sinistral	% neutral	% dextral	
04AED41	26	35	42	103	25	34	41	
04AED57	18	75	19	112	16	66	18	
04AED75	25	52	36	113	22	46	32	
04ALO24b	1	130	10	141	1	92	7	
04ALO25A	25	82	43	150	17	55	28	
04ALO30	45	87	63	195	23	45	32	
04ALO84	13	89	33	135	10	66	24	
04ALO102	10	101	18	129	8	78	14	
04ALO126	27	124	37	188	14	65	21	
04ALO129	30	92	29	151	20	61	19	
04APA4	35	117	62	214	16	55	29	
03APa2	24	125	40	189	13	66	21	
03APa81	34	124	47	205	17	60	23	
03APa97	32	111	36	179	18	62	20	
03APa111	17	90	33	140	12	64	24	

Sample 03APa2

Metagraywacke

Sample is 55% quartz

Shear sense: 66% no shear sense, 21% dextral shear, 13% sinistral shear

Very fine grained sample with clear pressure solution texture, many quartz crystals show evidence of grain boundary migration, biotite seen to grow next to quartz rich zones and grains, and is present throughout the matrix.

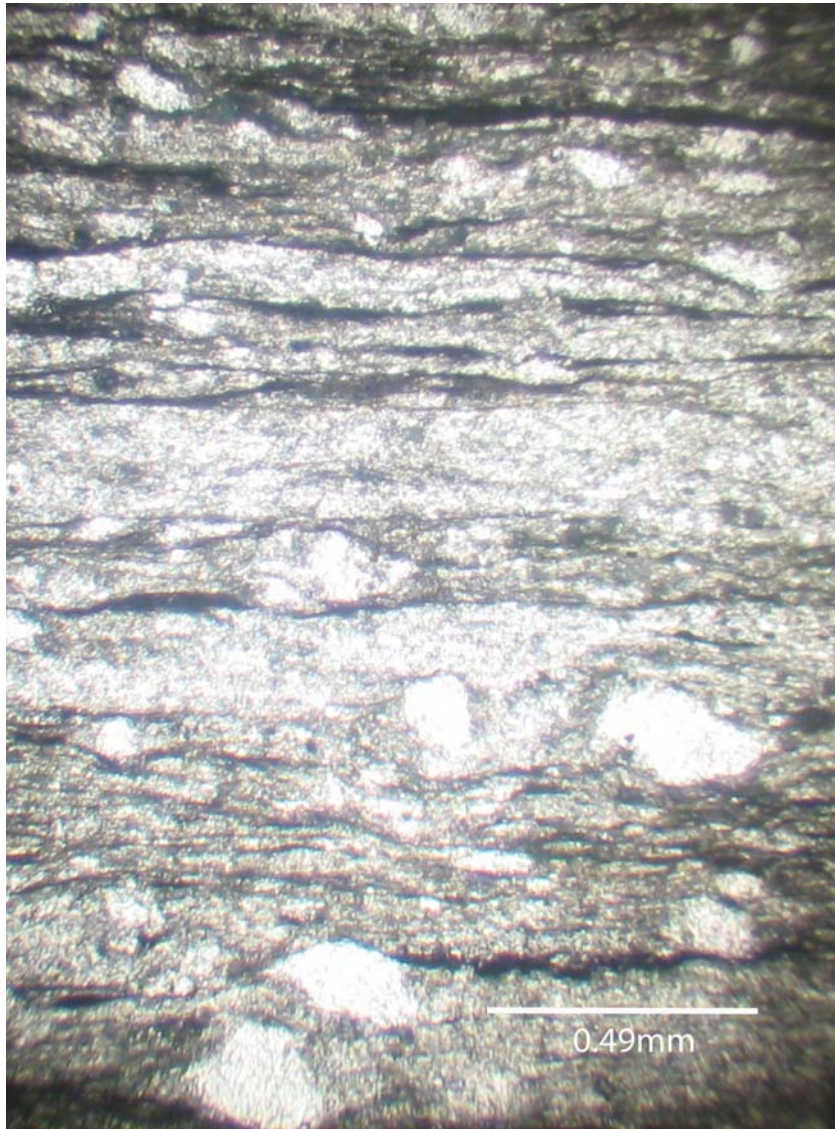
Sample 03APa81

Metapelite

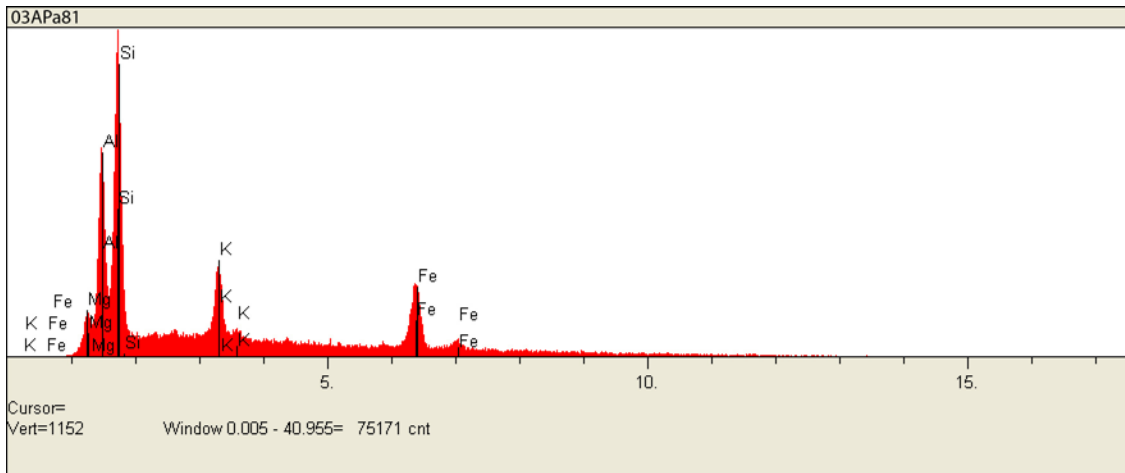
Sample is 35% quartz

Shear sense: 60% no shear sense, 23% dextral shear, 17% sinistral shear

This sample shows clear pressure solution texture. One can also see the relic texture of a fining upward sequence of the turbidity flows these rocks were originally created from (see photomicrograph below). Extinction of grains in fine grained matrix at 0° and 90° lead to the assumption that there may be micro-crystalline biotite in this sample. Analysis in the SEM confirmed that the micro-crystalline matrix contains biotite and other phyllosilicates (see spectrum plot of biotite below)



Plain light photomicrograph of fining up sequence in 03APa81.



Spectrum plot of biotite from sample 03APa81.

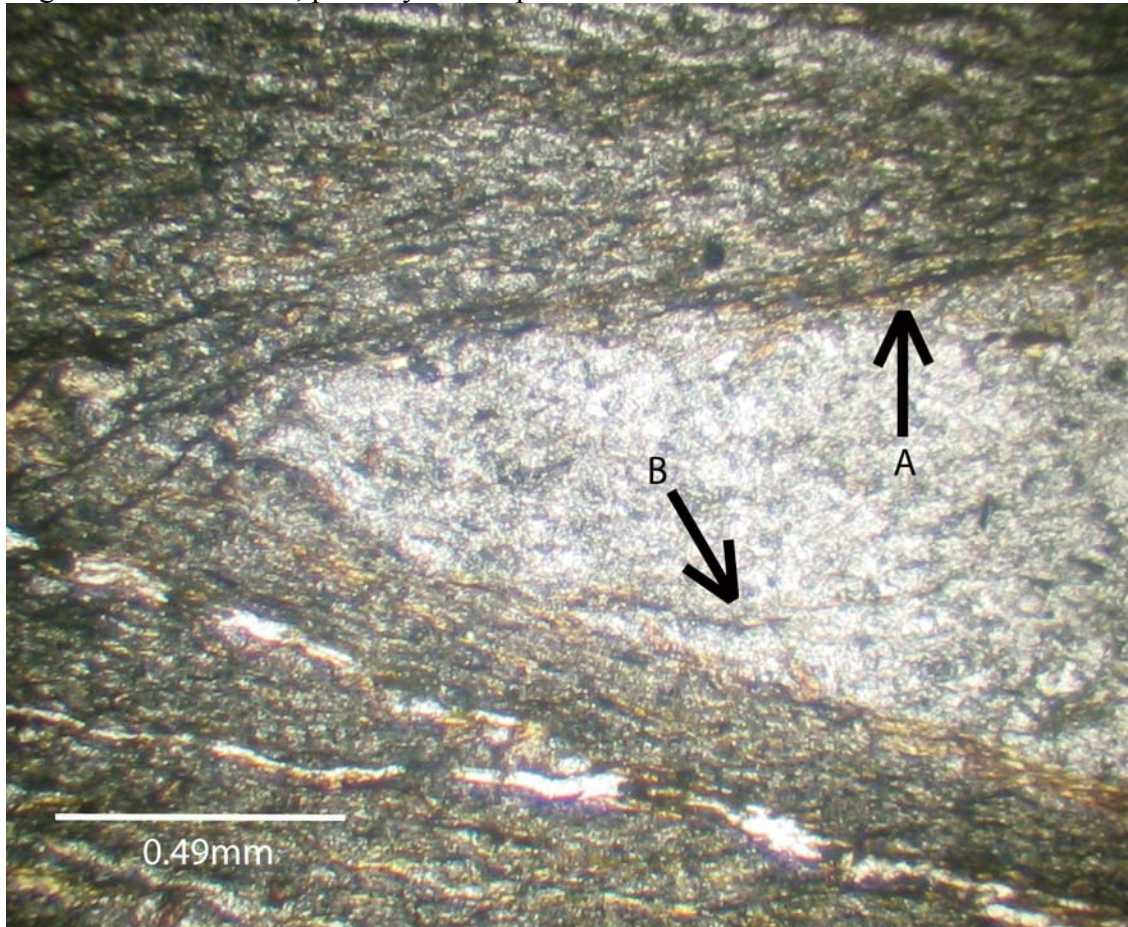
Sample 03APa97

Metapelite

Sample is 30% quartz

Shear sense: 62% no shear sense, 20% dextral shear, 18% sinistral shear

Clear pressure solution textures, highly veined, veins are truncated by the pressure solution showing a distinct volume decrease, biotites and other phyllosilicates form rinds around quartz rich zones and in microcracks (see photomicrograph below), some evidence of grain boundary migration within veins, possibly before pressure solution truncated the veins.



Plain light photomicrograph of 03APa97. A-Biotite forming rind around the edge of this stretched pebble. B-Biotite forming in and along a microcrack in the pebble.

Sample 03APa 111

Metapelite

Sample is 35% quartz

Shear sense: 64% no shear sense, 24% dextral shear, 12% sinistral shear

Distinct pressure solution texture in this sample shows clear s-c relation of a mylonitic rock from a dextral shear zone. Stretched and boudinaged micro veins. Biotite present.

Sample 04AED41

Metagraywacke

Sample is 65% quartz grains

Shear sense: 34% no shear sense, 41% dextral shear, 25% sinistral shear

The primary deformation mechanism observed in this sample was dynamic recrystallization seen as grains undergoing grain boundary migration. A possible remnant pressure solution texture can be seen in the growth pattern of biotite in this sample. Veins also show textures of crystal plastic deformation.

Sample 04AED57

Metagraywacke

Sample is 60% quartz grains and also has a quartz vein running through it

Shear sense: 66% no shear sense, 18% dextral shear, 16% sinistral shear

The matrix around quartz grains shows clear evidence of pressure solution. There is also evidence of grain boundary migration in larger quartz grains. Biotite is present.

Sample 04AED75

Metagraywacke

Sample is 60% quartz grains

Shear sense: 46% no shear, 32% dextral shear, 22% sinistral shear

Some evidence of remnant pressure solution textures in biotite growth patterns. In quartz rich areas there is evidence of grain boundary migration.

Sample 04ALO24b

Metagraywacke

Sample is 40% quartz grains

Shear sense: 92% no shear sense, 7% dextral shear, 1% sinistral shear

There is evidence of both pressure solution and dynamic recrystallization in this sample.

Pressure solution mostly associated with cracks and micaceous matrix in the sample. Filling many of the cracks there is a mineral with a high birefringence thought to be calcite or microcrystalline white mica.

Sample 04ALO25a

Metapelite

Sample is 30% quartz grains

Shear sense: 55% no shear sense, 28% dextral shear, 17% sinistral shear

Weak pressure solution texture that is stronger along cracks in the sample.

Sample 04ALO30

Metapelite

Sample is 10% quartz grains

Shear sense: 45% no shear sense, 32% dextral shear, 23% sinistral shear

Pressure solution is the dominant deformation mechanism.

Sample 04ALO84

Metagraywacke

Sample is 50% quartz

Shear sense: 66% no shear sense, 24% dextral shear, 10% sinistral shear

Crystal plastic deformation is obvious in this sample, with many examples of grain boundary migration. A few areas in the slide show pressure solution textures, these microcrystalline zones are thought to be small argillite rip-ups. Biotite growth throughout the slide looks to have grown along a pressure solution texture, though pressure solution textures are not pervasive through the sample.

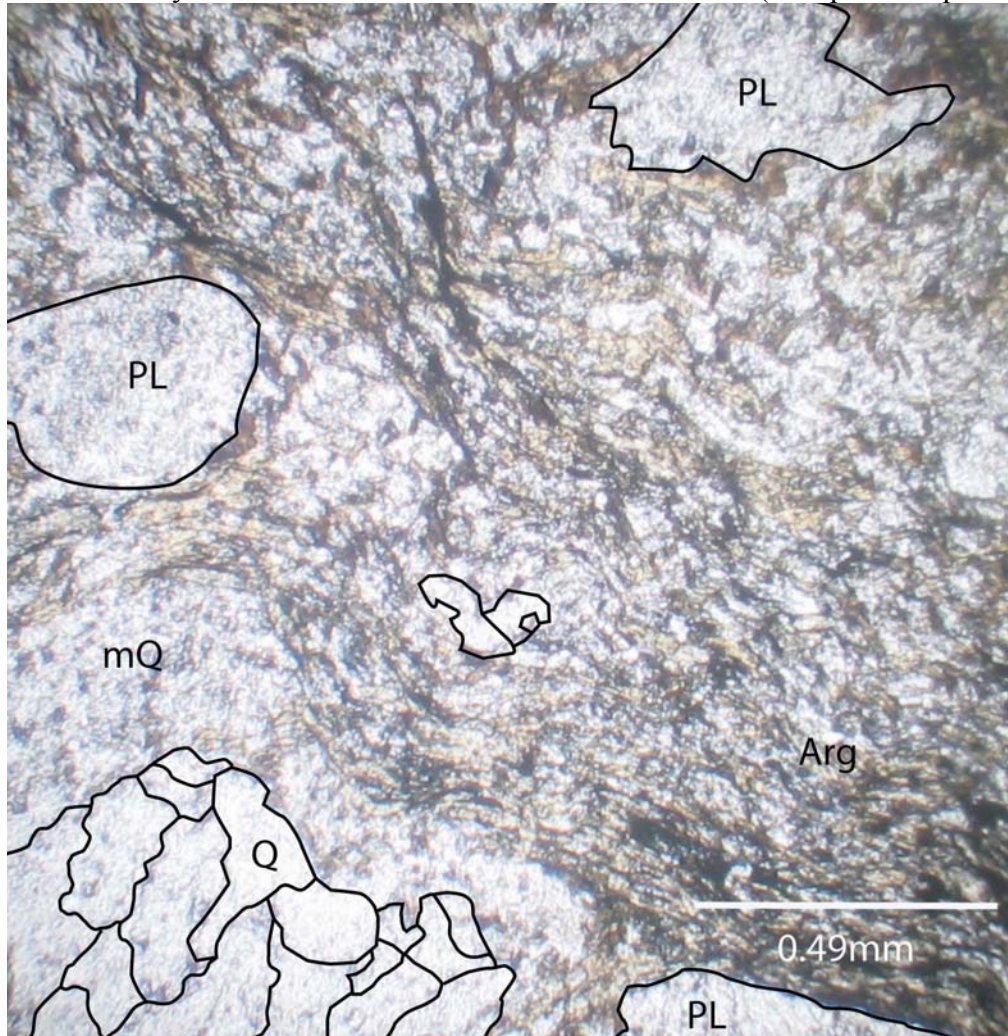
Sample 04ALO102

Metagraywacke

Sample is 55%

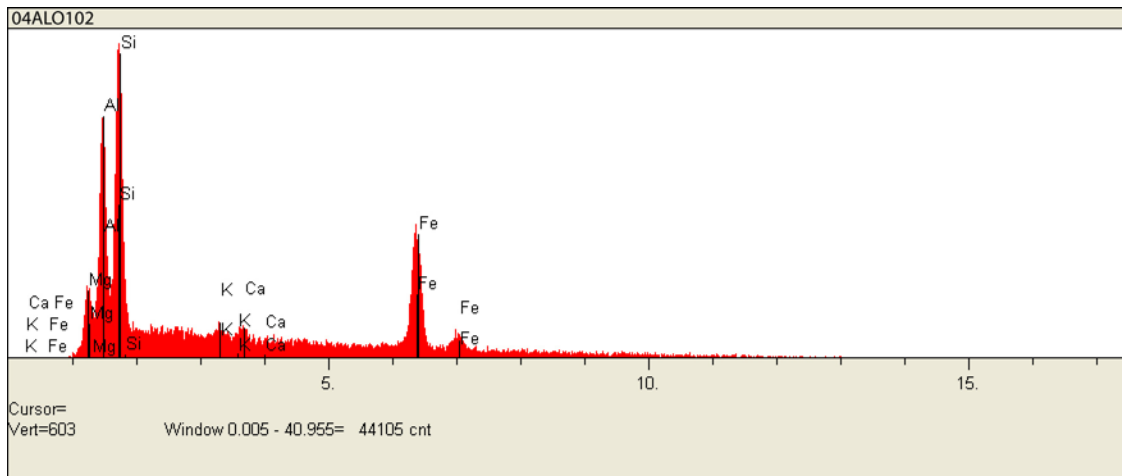
Shear sense: 78% no shear sense, 14% dextral shear, 8% sinistral shear

This particular sample showed both pressure solution and crystal plastic deformation textures. Grain boundary migration dominated the quartz rich zones of the sample; argillite rip-ups show pressure solution textures “snaking” through sample (see photomicrograph below). Argillite rip-ups have preserved biotite in the presence of chlorite. Under crossed polars chlorite looks blue, an SEM analysis shows that this mineral is in fact chlorite (see spectrum plot of chlorite below)



Plain light photomicrograph of 04ALO102. Arg-argillite rip up clast; Q-larger quartz grains showing irregular grain boundaries, undulatory extinctions observed under crossed polars; mQ-

zone of micro quartz also shows irregular grain boundaries and undulatory extinctions under higher power; Pl-plagioclase.



Spectrum plot of chlorite from sample 04ALO102.

Sample 04ALO126

Metagraywacke

Sample is 50% quartz

Shear sense: 65% no shear sense, 21% dextral shear, 14% sinistral shear

Under plain light this sample is clearly deformed by pressure solution. Some quartz rich zones look like they were stretched and truncated by pressure solution. Under crossed polars show distinct irregular grain boundaries and undulatory extinctions, evidence of grain boundary migration, which impairs clarity of pressure solution texture, indicating dynamic recrystallization occurring after pressure solution. Biotite is also observed to be growing between and around quartz grains.

Sample 04ALO129

Metagraywacke

Sample is 60% quartz

Shear sense: 61% no shear sense, 19 % dextral shear, 20% sinistral shear

Clear pressure solution texture with some biotite growth. Some localized examples of grain boundary migration.

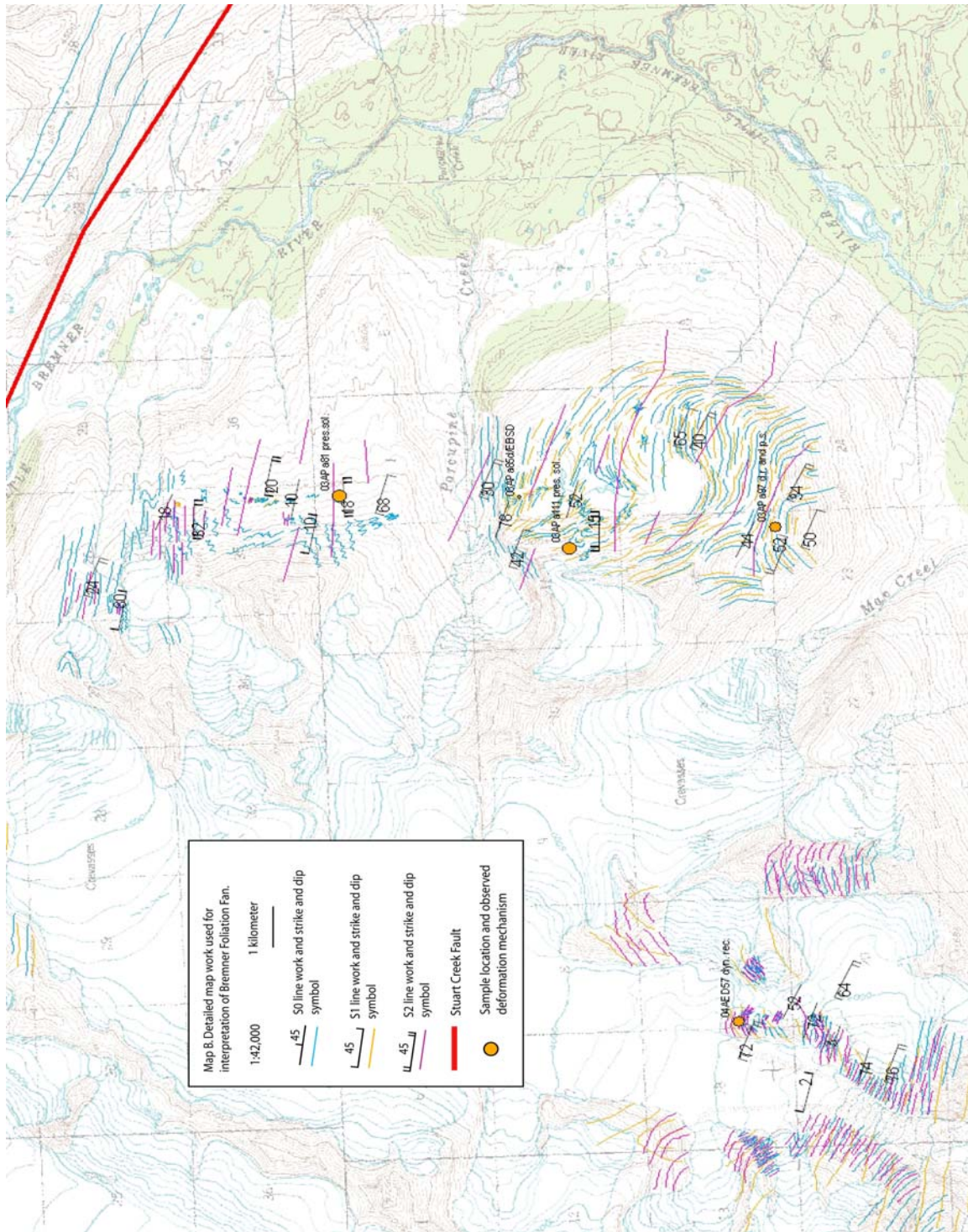
Sample 04APa4

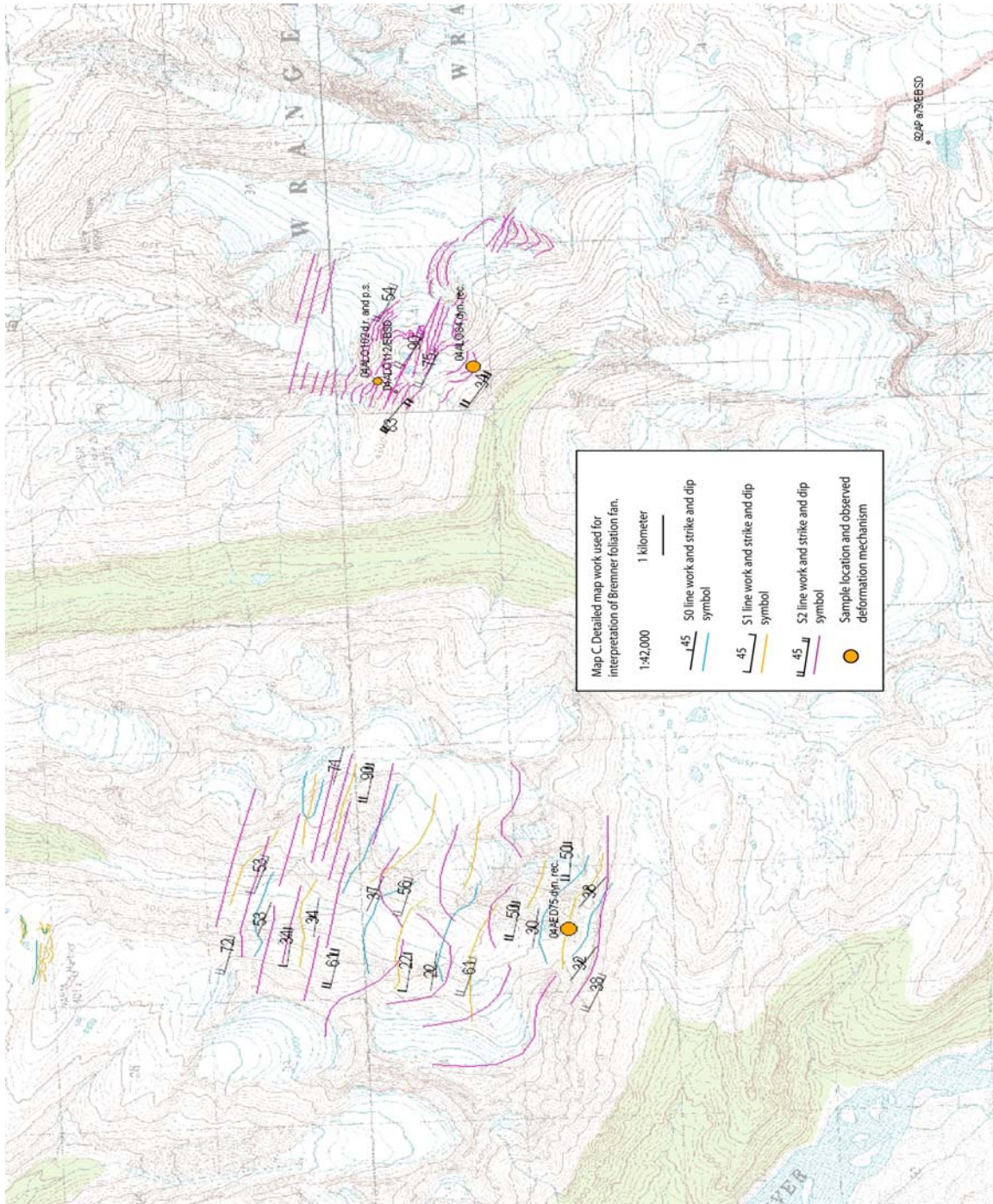
Metapelite

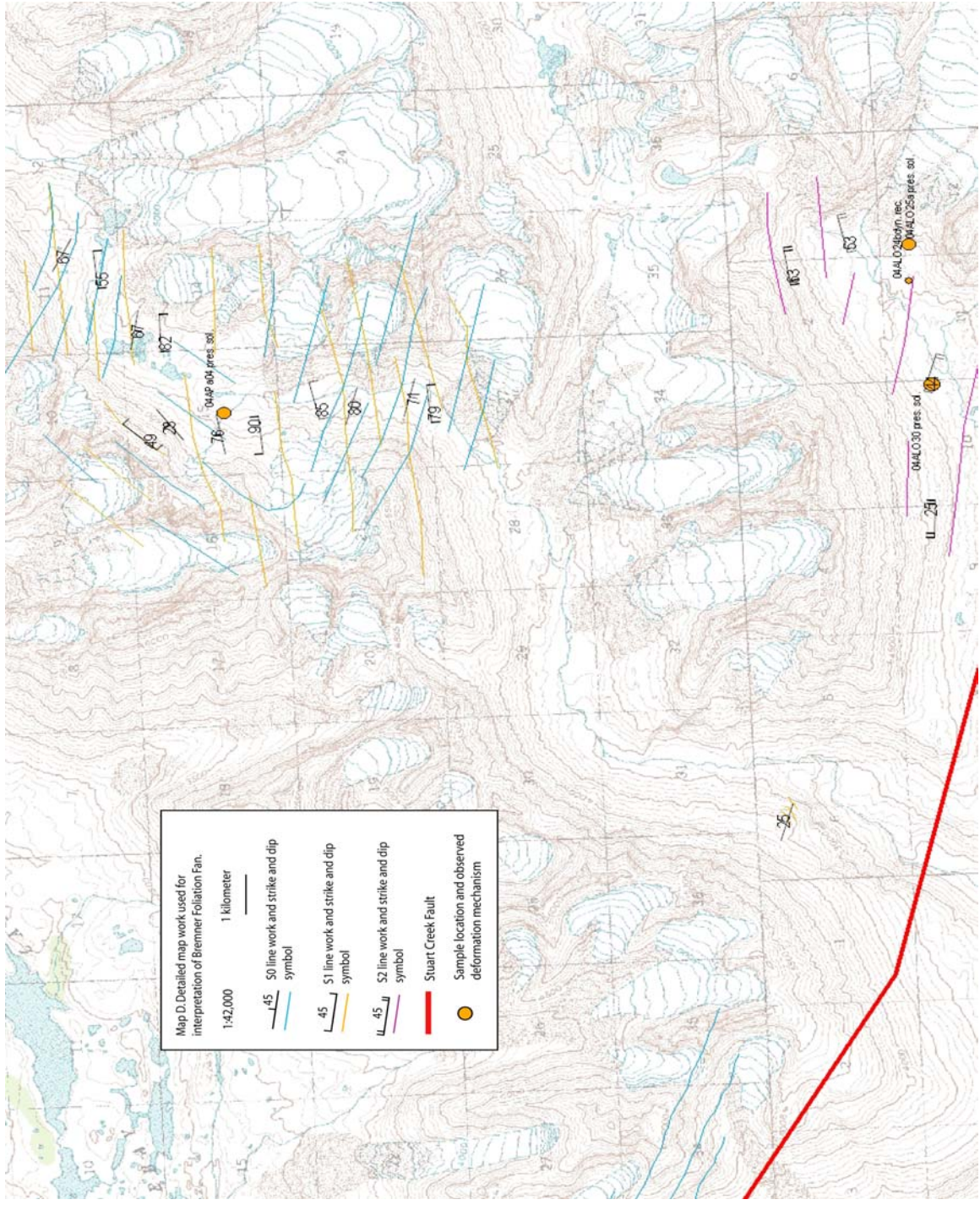
Sample is 10% quartz

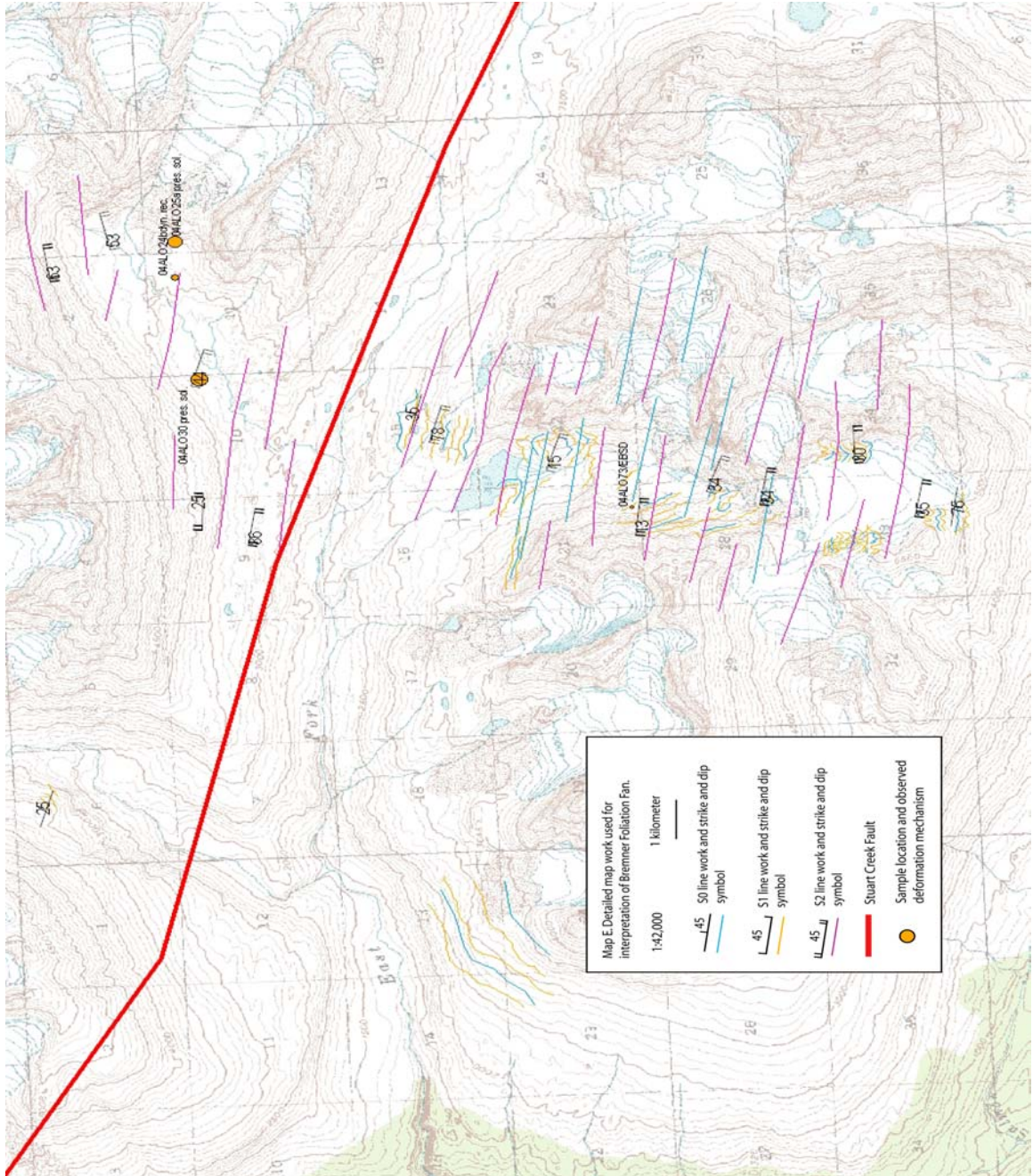
Shear sense: 55% no shear sense, 29% dextral shear, 16% sinistral shear

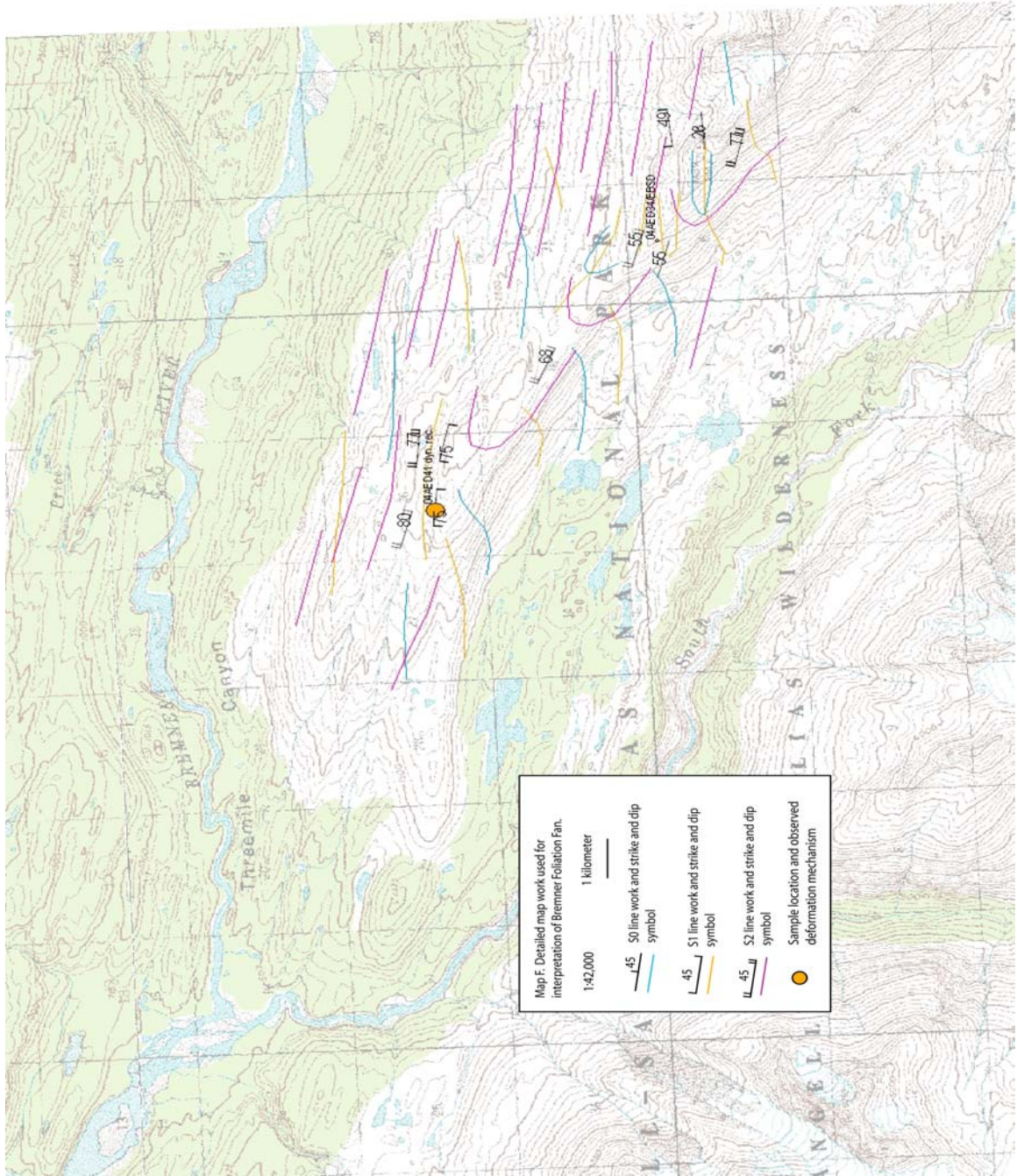
Clear pressure solution texture, contains high birefringent mineral possibly calcite, or microcrystalline white mica.











VITA

Erik Michael Day was born March 17, 1981 in Cheshire, CT to his parents Grant and Marta Day. He graduated from Cheshire High School (1999) and Occidental College (2003). Erik is planning on continuing his education and working towards a Ph.D. in tectonics and structural geology.